The Thesis Committee for Rameshwar Sreenivasan
Certifies that this is the approved version of the following thesis:

Sustainability and Thermal Aspects of Polymer based Laser Sintering

APPROVED BY

SUPERVISING COMMITTEE:

Supervisor: _____

David L Bourell

_____

Joseph J Beaman

Sustainability and Thermal Aspects of Polymer based Laser Sintering

by

Rameshwar Sreenivasan, B.E.

Thesis

Presented to the Faculty of the Graduate School of

The University of Texas at Austin

in Partial Fulfillment

of the Requirements

for the Degree of

Master of Science in Engineering

The University of Texas at Austin

December 2010

Dedication

For Sreenivasan K P

Acknowledgements

The author wishes to express his deepest thanks to his advisor, Dr. David L. Bourell, for providing this research opportunity and for guidance, motivation and support throughout the completion of this work.

The author is indebted to the Department of Defense. The thermal distribution study was sponsored under Grant #GRT00015778.

The author is also grateful for the services provided by Mark Phillips, technical assistant of the LFF laboratory in the Mechanical Engineering Department, UT Austin.

The author also wants to thank Bharadwaj Muralidharan for helping him with LabVIEW tutorials. His services were instrumental in designing the LabVIEW circuits for the entire study. The author also wants to thank all his friends who have provided the necessary impetus.

The author is indebted to many others for providing support and encouragement. Above all, he is thankful of his parents for providing for everything in his life.

RAMESHWAR SREENIVASAN

The University of Texas at Austin

December 2010

Sustainability and Thermal Aspects of Polymer based Laser Sintering

by

Rameshwar Sreenivasan, M.S.E.

The University of Texas at Austin, 2010

Supervisor: David L Bourell

Additive Manufacturing (AM) processes which include Selective Laser Sintering (SLS) have experienced tremendous growth and development since their introduction over 20 years ago. It becomes highly important at this stage to evaluate the sustainability of the process and refine it to reduce energy and material consumption. In this study, a sustainability analysis was performed on the SLS process with Nylon-12 using the Environmental and Resource Management Data (ERMD) known as Eco-Indicators. The energy perspective alone was considered and a Total Energy Indicator (TEI) value was calculated using various parameters to quantify process sustainability: process productivity, energy consumption rate, etc.

Precise thermal control of selective laser sintering (SLS) is desirable for improving geometric accuracy, mechanical properties, and surface finish of parts produced. An experimental setup to monitor the temperature distribution was designed using Resistance Temperature Detectors (RTD) as a part of this study. Discrepancies in

temperature profiles were investigated and recommendations were made to improve thermal characteristics of the SLS process.

Table of Contents

List of Tables

List of Figures

Chapter 1

INTRODUCTION AND BACKGROUND

1.1. Sustainability

1.1.1 Sustainability-Definition

The United Nations (UN) Conference on the Human Environment (Stockholm, 1972) added the environment to the UN's list of global problems which resulted in the creation of the United Nations Environment Programme (UNEP). The 1972 report titled 'The Limits of Growth' warned that the earth's natural resources were being quickly depleted and that there might not be resources remaining to allow the developing world to industrialize [1].

The report 'Our Common Future' [2] was released in 1987 by a UN commission chaired by the Norwegian Prime Minister, Gro Harlem Brundtland, and the concept of "sustainable development" was adopted. Sustainability is defined here as the design of human and industrial systems to ensure that humankind's use of natural resources and cycles do not lead to diminished quality of life due either to losses in future economic opportunities or to adverse impacts on social conditions, human health and the environment. These requirements reflect that social conditions, economic opportunity, and environmental quality are essential if society's development goals are reconciled with international environmental limitations. Accordingly, fundamental research, education, and knowledge transfer are needed to meet this vision [1].

The point of view, according to the report, is that the present wasteful lifestyle of the developed nations is not sustainable on account of their disproportionately large per capita resource consumption that results in environmental degradation and societal inequity. In fact, some scholars have estimated that supporting the present standard of living seen in the developed nations for all mankind with the current technologies requires the natural resources of two additional Earths [3].

The rallying wisdom behind sustainable development, therefore, is for restraining the rate of use of material and nonrenewable energy now so as to keep enough for many future generations to fulfill their own ambitions of living standards. This could be possible by adopting technologies that are four times as resource-efficient as the current ones. This is called the Factor 4 idea, in contrast to the previous assertion of the Factor 10 idea that advocated the need for improving the efficiencies by an order of magnitude. Thus, sustainable development is thought to be a wise balance among economic development, environmental stewardship, and societal equity. In some business circles this is referred to as the triple bottom line.

A consensus “straw man” definition that a group of professionals from various scientific, engineering, economic, and ecology backgrounds at the United States Environmental Protection Agency’s (EPA) National Risk Management Research Laboratory suggested is that sustainability occurs when the material and social conditions for human health and the environment are maintained or improved over time without exceeding the ecological capabilities that support them [3]. Therefore, sustainability can

be thought of as the goal, with sustainable development, as the process for achieving it. Figure 1 illustrates the concept of sustainability.

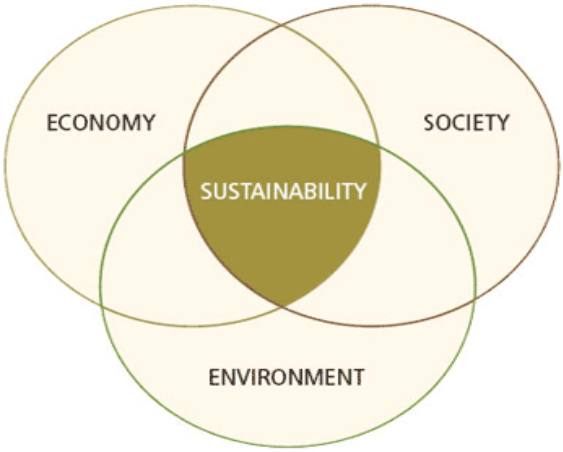

Figure1- Illustration of Sustainability [2]

If it is accepted that the Earth's nonrenewable resources decline with uncontrolled economic development, one is forced to conclude that the best one can do is to considerably slow down this decline to meet the challenges posed by population growth and inevitable development. This is clearly possible since the advancement of science and technologies has provided steadily increasing energy and material efficiencies in producing goods and services. The 'Our Common Future' treatise on sustainability centered on global conditions of ecology (i.e., environment), economic development (i.e., by technologies), and societal equity [3]. Based on this, the definition for sustainability is as follows. Sustainability is defined as a measure of degree with which the material and social conditions for human health and the environment are maintained or improved over time without exceeding the ecological capabilities that support them [3].

1.1.2 Sustainability Indicators

Another important need is the definition of sustainability indicators that encompass key issues and are quantifiable. Unfortunately, less work has been performed on sustainability indicators than other indicators. Figure 2 illustrates that the selection of sustainability indicators should include considerations related to economics, society, and the environment. The International Institute for Sustainable Development has been working on a set of indicators since 1995 to measure progress toward sustainable development [1].

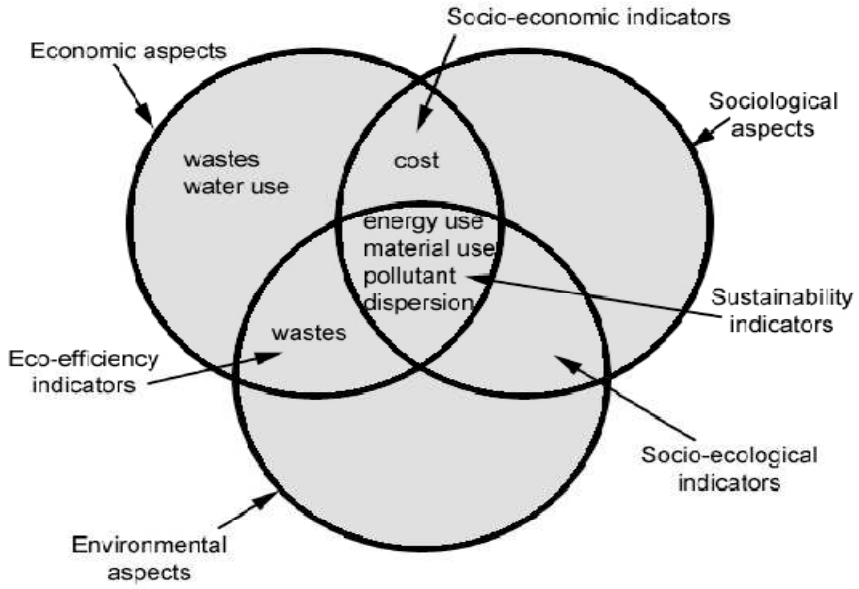

Figure 2- Sustainability Indicators [2]

A great deal of progress has been made in the development of methods for Life Cycle Assessment (LCA) to allow evaluations of environmental impacts across all stages

of product production and use. As shown in Figure 3, these stages include the extraction of natural resources, manufacture, product use, and reuse, recycle or disposal. Figure 3 shows that product evolution through the life cycle (clockwise) involves material and energy use, releases to the environment, and associated costs (private and societal). In most cases, the inner loops of reuse and remanufacturing are preferred, requiring less raw materials, energy, time, and cost. These efforts to invoke LCA have been successful at reducing waste, pollutants, and energy use for a number of industries [1].

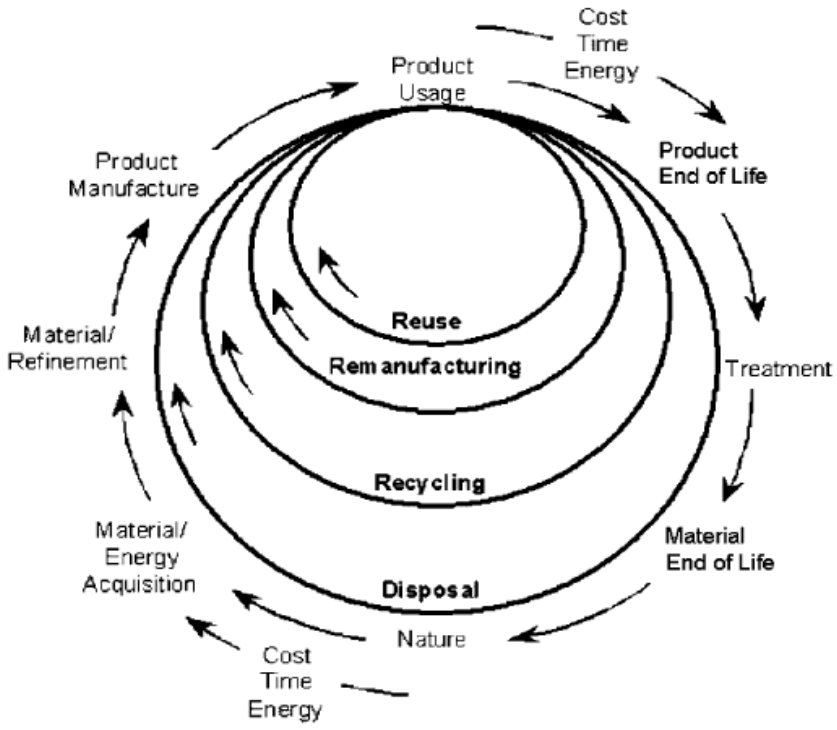

Figure 3- Life Cycle stages of Process [1]

On the side of product design, considerable effort has been undertaken to develop the concepts, methodologies and implementations of product lifecycle, end of lifecycle

factors, and even multi-lifecycle issues. However, processes are much more universal than products, and a successful process design often has great importance to and great staying power for an entire industry, More recently, focuses on studying process level environmental performance have been developed, particularly for conventional machining processes [3].

Two classes of metrics are in development to indicate the state and performance of a system. These metrics are more popularly known as indicators. Those that indicate the state of a system are known as content indicators and those that measure the behavior of a system, performance indicators.

Naturally, researchers have attempted to measure improvements in terms of three groups of metrics corresponding to the three aspects of sustainability: ecological metrics, economic metrics, and sociological metrics. These metrics measure only one aspect of the system, and, therefore, are one-dimensional (1-D). There have been attempts to measure 2-D aspects as well [3].

These 2-D metrics are shown in Figure 2 as belonging to the interactions of any two aspects of sustainability. Thus, one can identify eco-efficiency metrics, socio-ecological metrics, and socio-economic metrics. 3-D metrics can be obtained from the intersection of all three aspects, which could be called true sustainability metrics. These seven types can be summarized below:

Group 1 (1-D): economic, ecological, and sociological indicators

Group 2 (2-D): socio-economic, eco-efficiency, and socio-ecological indicator

Group 3 (3-D): sustainability indicators

Dozens of indicators have been suggested for use in determining improvements made to chemical processes, a manufacturing site, or a manufacturing enterprise. One of the significant studies on sustainability metrics was sponsored by the Center for Waste Reduction Technologies of American Institute of Chemical Engineers (AIChE) for evaluating process alternatives [3]. The metrics or indicators used in this study were material utilization, energy use, water use, toxics dispersion, pollutant dispersion, and greenhouse gas emission—all either per unit mass of product or alternatively per unit of economic value addition. Given the values of these indicators for two or more processes for a product, a value judgment was made for the preferred approach. The other significant effort was made under the auspices of the Institution of Chemical Engineers (IChemE) in the U.K. In this effort, the indicators were specifically grouped into environmental, economic, and social categories. Theirs was a comprehensive list of all possible indicators that might be relevant to a manufacturing site. The environmental indicators were further shown as belonging to either resources or environmental impact categories. Among resources the important indicators that this study suggested were energy use, material use, water use, and land use; and among environmental impacts, acidification, global warming, human health, ozone depletion, photochemical smog formation, and ecological health. Economic indicators include several value-added measures and R&D expenditures. Lastly, a range of social indicators had been proposed that were based on employee benefits, safety, and how the employees are treated in the

workplace. The only known study in the open literature on 2-D metrics development is that of BASF, the chemical company [4], although numerous process improvement methods have been developed that address eco-efficiency issues. BASF created the eco-efficiency indicators to measure the environmental and economic performance of a product or a process. In the BASF method, five ecological indicators were combined to provide an "ecological footprint", which was plotted against the life cycle cost of process options, and the process that has the lowest of both was judged to have superior eco-efficiency [3].

Identification of true sustainability indicators (i.e., 3-D), would more fully reveal sustainability features than the 2-D and 1- D indicators, all of which may or may not be equally important, especially at the beginning of an assessment.

This idea calls for measuring the 3-D indicators first, and, if decision-making needed further elaborations, explores the 2-D and 1-D indicators, as well to address certain issues as might be important in specific situations. Because of the large variety of manufacturing cases that are possible to consider, the determination of 3-D indicators would be necessary, but not sufficient.

To identify the true 3-D indicators, the main concerns are ecological impact, economic development, and societal equity. Those indicators that directly affect these three concerns simultaneously are 3-D. Those indicators as shown in Figure 2 are

i) Nonrenewable energy use

ii) Material use

iii) Waste generation

iv) Pollutant dispersion

v) Clean water use

vi) Cost

Energy is the prime driver for economic growth, and if nonrenewable, always has an ecological impact through the emission of pollutants and greenhouse gases, and, since limited, does affect future generations. It would appear that nonrenewable energy use is inherently a 3-D indicator. Likewise, material use can have direct ecological impact, is associated with value creation, and can have intergenerational impact. Thus, material use is also a 3-D indicator. Process wastes that are well controlled and contained are economic value-losses and are 1-D economic indicators. Some wastes, such as gypsum piles, could, however, be 2-D eco-efficiency indicators, the effect being environmental nuisance and potential pollution. Pollutant dispersion is a 3-D indicator, as it represents environmental impact, has economic cost associated with it, and, frequently, has a bearing on the health of the people and ecosystems in the neighborhood of the manufacturing units. The cost of manufacturing is a reflection of the nature of technology (economic value creation) and affordability for public consumption (societal value)—thus, a socio-economic indicator. In comparison, among manufacturing processes for a product, the lowest cost is not only desirable to the manufacturer for its profitability, but also intricately connected to the satisfaction of the customers. In this line of thinking, sustainable process design is a multiobjective optimization in which the cost of

manufacture is minimized while improving all 3-D indicators in the first step of the design endeavor.

1.1.3 Industrial Ecology

The broad sense of sustainability can be limited to engineering under the term ‘Industrial Ecology’. The study of the flow of materials and energy through industry and implications for the overall production of products and waste is termed Industrial Ecology [IE]. Recently, the approach of industrial ecology has been expanded further to consider material and energy flows from multiple, often inter-related industries, and through local environments, regions, national economies, and global trade [1].

Generally, IE involves both processes and products. The interaction of process design with the environment concerns is somewhat different from that of product design. The IE interaction is thus heavily influenced by two rather separate groups of designers.

Depending on content, IE, is also referred to as Green Manufacturing [GM], clean manufacturing, Environmentally Conscious Manufacturing (ECM), Environmentally Benign Manufacturing (EBM), Environmentally Sound Manufacturing (ESM). It is instrumented in the recognition of industrial impacts on the environment, development of methods for their measurement, and assessment of pollution extent from various industries. The main idea behind IE is the integration of the manufacturing industry with nature, and it was suggested that if symbiotic, closed-loop links could be established, the negative impacts of industrial activities would be significantly reduced. However, the

existing gap between industrial expansion and environmental concern renders the implementation of IE difficult in practice. On the one hand, GM has become an important issue in industry, driven by the regulations governing manufacturing emissions and end-of life disposal of products, increasing demand for environmental certification requirements (ISO 14000) worldwide and an emerging consumer preference for “green” products. On the other hand, there is still a significant confusion and misunderstanding about its components, costs, benefits and implementation [5].

Much has yet to be done to be able to incorporate the vision of GM into the constant need for industrial growth. The first step towards achieving this goal is gaining better understanding of the environmental impacts of both current and newly developed industrial activities and identifying their extent. Environment Conscious Production (ECP), Environment Conscious Design (ECD), materials recovery and recycling, product recovery and remanufacturing, as well as collection and disassembly each have their role in the life cycle of the product processing. However, to date, the extent of the corresponding environmental impacts of the product processing lifecycle stages has not been fully quantified [6].

1.1.4 Sustainability issues in Conventional Manufacturing

Any manufacturing process that involves material removal due to mechanical stresses exceeding the strength of the material, induced by a tool is referred to as a conventional machining process [7]. The forming and shaping of metals and plastics, via processes such as injection molding, stamping, and forging, are essential to modern society. Tools, dies, and molds, collectively referred to here as ‘‘tooling,’’ are required to produce nearly all plastic and metal products in industries such as automotive, medical, aerospace, and consumer electronics.

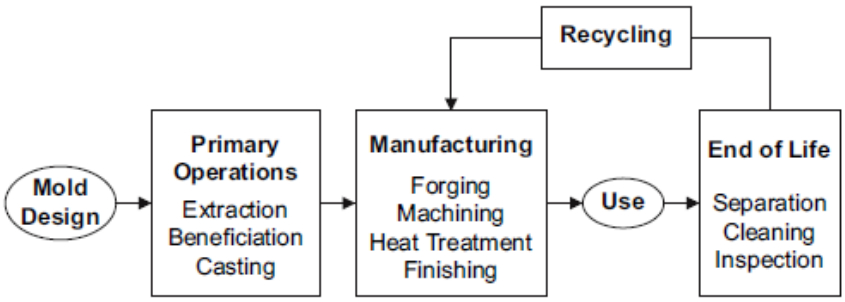

Figure 4-Major components of the tooling life cycle

The tooling life cycle (Figure 4) is not environmentally sustainable for a number of reasons, including the consumption of limited material and energy resources and the pollution of terrestrial, aquatic, and atmospheric systems during production and utilization activities. The manufacturing operations generating these impacts include casting, forging, and machining, operations which, according to the U.S. Environmental Protection Agency [2], release a significant percentage of the nation’s greenhouse gases,

consume large amounts of limited natural resources, are among the most significant polluters of freshwater systems, and are responsible for the release of particulates, metal oxide fumes, and respirable organics that are harmful to human health. In addition to material, energy, and associated emissions, pollution in the tooling production cycle can be attributed to ‘‘engineered scrap’’ operations such as machining that removes metal previously invested in the life cycle of the tool, and ancillary products and materials (e.g., hydraulic oils, cutting fluids, casting sand, cutting tools, etc.) that are necessary to achieve economical tooling production but that are not part of the final tool itself. These externalities of production are significant inhibitors to the goals of environmentally benign manufacturing, creating opportunities for cleaner production and progress towards sustainability [8]. Table 1 gives a list of opportunities to reduce the environmental burden while dealing with conventional manufacturing processes

In 2002, the overall injection molding energy consumption in the U.S. in a yearly basis amounted to 2.06×10^8 GJ. This value included all steps in the LCI, except polymer production. Including polymer production would increase this number by an order of magnitude. This value (2.06×10^8 GJ) was of similar magnitude to the overall U.S. energy consumption for sand casting (1.62×10^8- 2.28×10^8 GJ) [9]. To comprehend the scale of the U.S. injection molding energy consumption, Table 2 provides values of the entire electricity production of several countries in 2002. Without accounting for the electric grid, the overall injection molding energy consumption in the U.S. amounts to 6.19×10^7 GJ/year. This value can be compared with the values in Table 2. It seems

imperative for industry to keep improving the efficiency of the process, since small savings anywhere in the LCI can lead to tremendous energy savings on a national scale. This seems an intelligent move in a time of rising energy prices [9].

Process	**Opportunities for reduced Environmental burden**
Casting	Air/Water emissions and energy consumption from furnace and mold material handling operations; solid waste from discarded mold material; general footprint of factory operation and associated overhead.
Forging	Energy Consumption; hydraulic fluid use and spills; conversion coating use; metal working lubricants and fluids; footprint overhead; tool production and disposal.
Machining	Energy Consumption; production and handling of waste chips; metal working fluids; tool production and use; on-site water treatment

Table 1-Tooling supply chain manufacturing operations and associated environmental impact [4]

Countries	GJ/Year
Afghanistan	1.71E+06
Guatemela	2.22E+07
Honduras	1.37E+07
Iceland	2.84E+07
Jamaica	2.26E+07
Jordan	2.55E+07
Nicaragua	8.41E+06
Nigeria	6.25E+07
Panama	1.78E+07
Slovenia	4.29E+07

Table 2-Countries with smaller order of magnitude electricity production to the amount of energy spent injection molding in the U.S [9]

1.1.5 Additive Manufacturing

Additive Manufacturing (AM) is a 'What you see is what you get' process where the virtual model and the physical model are almost identical [10].

With additive manufacturing, the machine reads in data from a CAD drawing and lays down successive layers of liquid, powder, or sheet material, and in this way builds up the model from a series of cross sections. These layers, which correspond to the virtual cross

section from the CAD model, are joined together or fused automatically to create the final shape. The primary advantage to additive fabrication is its ability to create almost any shape or geometric feature.

Additive Manufacturing (AM) can be used not only to generate rapid prototypes for design optimization and verification but also to create production tools or directly fabricate products. This relatively new manufacturing technology has been experiencing tremendous development and growth since its introduction a little over two decades ago. AM has been widely adopted in aerospace and automotive industries, and is quickly becoming an important production process in electronics industry.

1.1.6 Sustainability in Additive Manufacturing

In view of the fast growth and wide adoption of various AM processes, it is important to study the lifecycle performance of AM processes, including consumption of natural resources and energy, and impact on human health and the environment, together with other process attributes such as cost, accuracy, productivity, and functionality, so that the AM technology can become more sustainable.

In general AM processes have many good environmental characteristics. The material utilization rate is much higher in material additive process adopted in AM than in material removal process used in machining process. The waste streams are less in AM processes than in conventional manufacturing processes such as machining. Worn tools and scrap seldom occur in AM processes and equipment. Cutting fluids, which are the

major source of hazard in machining, are not used in AM processes. Comparing with conventional manufacturing processes, AM processes have distinguishing features in process mechanisms, materials, energy use, etc. [11]

AM operations were highlighted at the September 2001 Workshop on Environmentally Benign Manufacturing (EBM) for their potential to reduce environmental impact within the metals manufacturing industry. In contrast to metal removal operations conventionally used in the tooling industry, an additive process creates a mold or die cavity by 'building the boundary' instead of removing cavity material from a bounding volume. By utilizing only the amount of material needed for the product, additive manufacturing technologies have the potential to reduce the life cycle material mass and energy consumed relative to conventional subtractive techniques by eliminating engineered scrap, while also eliminating the use of harmful ancillary process inputs. Certain AM techniques also have the capability to completely eliminate supply chain operations associated with the production of new tooling by their capability to enable repair and remanufacturing of obsolete or failed tooling [4].

Many CNC machined parts are produced from billet. In some cases the volume of this billet can be significantly more than the part that is to be produced. Within the aerospace sector this is called the buy-to-fly ratio. It is not uncommon for ratios of 20:1 to be experienced. In other words, for every 20 Kg of raw material purchased as a billet, only 1 Kg of material ends-up in the final part. This means that 19Kg of cutting chips (swarf) becomes a waste stream and finds its way back into the materials supply chain.

For low cost and low melting temperature materials such as aluminum, this is not a significant issue. However, for more expensive and higher melting temperature materials, such as titanium, which is prevalent in aerospace, this is becoming a significant economical and logistical problem. Moreover, titanium billet stock is not readily accessible with significant lead times of up to and over 12-months [12].

Inversely, direct metallic AM process are highly material resource efficient, as they only use the raw material required to consolidate the final part, and in some cases a small amount of support structure [12]. Moreover, any material that is not consolidated during the ALM process can be re-used in the machine, without entering into the recycling supply chain. This material utilization factor has a number of significant business benefits. Figure 5 shows a typical ALM part made using Electron Beam Melting. This part would have a very high material waste ratio if manufactured using CNC machining.

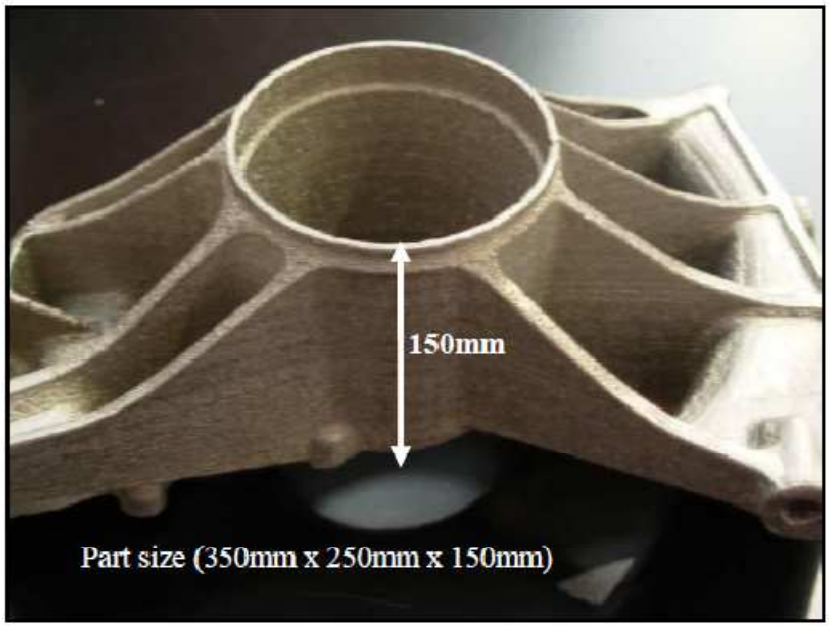

Figure 5-Electron Beam Melted component part with high materials waste ratio when made using CNC machining [12].

In terms of carbon footprint reduction, it is suggested that there are five primary environmental and sustainability benefits to the adoption of additive manufacturing [12].

1. Reducing the amount of raw material required in the supply chain. Hence, reducing the need to mine and process primary material ores.

2. Reducing the need for energy intensive and wasteful manufacturing processes such as casting, or processes such as CNC machining which require cutting fluids.

3. By enabling the design of more efficient products with better operational performance such as hydraulic components with conformal fluid paths.

4. By reducing the weight of transport related products that go on to contribute towards the carbon footprint of the vehicle into which they are integrated.

5. By allowing parts to be manufactured closer to the point of consumption by eliminating the need for fixed tooling and centralized manufacture [12].

A variety of industrial sectors have found remanufacturing of existing products, in lieu of original production, a successful approach to simultaneously reduce costs, increase productivity, and reduce environmental impacts. While it has been estimated that such remanufacturing activities account for $56 billion of the U.S. economy per annum, remanufacturing of tooling is rarely performed. This is because currently used techniques such as welding cannot restore metal microstructures to ‘‘as-new’’ condition when the tool fails or a design change occurs. However, recent scientific and engineering advances in laser-based metal freeform fabrication have put tooling remanufacture within the reach of technological and economic feasibility. For the tooling industry, remanufacturing enabled by certain AM techniques provides an excellent opportunity to increase industrial competitiveness by reducing tooling costs and lead times relative to original production. By eliminating polluting steps in the supply chain for new tooling production via remanufacturing, AM offers an opportunity to increase industrial competitiveness while reducing environmental impacts [8].

1.1.7 Sustainability Analyses of Additive Manufacturing Technologies

Though AM offers various sustainability advantages compared to conventional manufacturing techniques, It is essential to look into these processes, investigating how the process variables influence the environmental consequences, and apply a systematic method to assess the process environmental performance so that these processes can be optimized with consideration of their environmental properties [5].

LCA has been found useful for examining the design of products and processes to reduce the impact upon human health and the environment and to achieve sustainable industrial development. The first stage in any process is extraction/production of raw material. Then it undergoes refining to be transformed into a form suitable for various manufacturing processes. A part produced with an AM process generally goes through the following stages:

(a) Inputting the building material into the system,

(b) Building the part layer by layer

(c) Shape replication and sintering or burning (for tooling processes) and

(d) Post-processing.

When the user finishes using the part fabricated by AM, the part goes to the disposal stage: to be land-filled, incinerated, or recycled. While the material, part usage and part disposal are not exactly part of a process, their inclusion provides a holistic view of the environmental performance of an AM process. Thus, factors taken into account in

process environmental performance include the material extraction stage, energy consumption and process wastes in the fabrication and replication stages, and the disposal stage. In the material preparation stage, the environmental impact is material extraction and production. During the part building stage, the main environmental impact is energy consumption. The environmental performance value obtained should provide an unambiguous measure for the combined environmental impact of material, process, energy, etc. This kind of data quantifies the impact of the process to the environment. It should be noted that there is no database of this kind available today [5].

1.1.8 Objective of this study

The primary objective of this study is to evaluate the sustainability of Selective Laser Sintering (SLS) of Nylon-12 from an energy perspective and to identify the energy drains of the process. Energy consumed by individual components of an SLS machine is measured and a quantification of sustainability of the process is provided. The sustainability of other manufacturing processes is also investigated and a comparison is made between SLS and other processes. Finally, recommendations on how to improve the sustainability of an SLS process are made.

1.2 Thermal Distribution in SLS

The selective laser sintering process is primarily a thermal process as the object is formed by sintering or fusing of powder at selected locations of a layer that receive directed energy from the laser sufficient to reach the fusing or sintering temperature . Those portions of each powder layer that do not receive the laser energy remain unfused and thus remain below the fusing or sintering temperature. In addition, the temperature of the powder receiving the laser energy will generally be higher than the temperature of underlying prior layers (fused or unfused). As such, significant thermal gradients are present at the target surface of the powder in the SLS process.

It has been observed that these thermal gradients result in distortion of the object being produced, thus requiring thermal control of the SLS process for the objects produced to precisely meet the design [13].

Typically inaccuracies in the selective laser sintering process using polymer materials occur due to inhomogeneous shrinkage during the building and cooling processes, which induce stresses and result in distortion of the laser-sintered parts. Temperature measurements performed within an SLS machine in the past have shown a strong temperature gradient in the x-y plane of a layer, thus making the shrinkage of geometry, dependent on its x and y positions in the build room. Yet part shrinkage does not only depend on the temperature at which the part is subjected to laser sintering, it is

also impacted by cooling, i.e. the length of time the powder bed retains heat, and by the thickness of the powder layer.

The temperature distribution within the part bed and the changes in temperature during the building and cooling processes differ with the geometry of each part to be produced. The reason for this lies in the variation in the energy applied by the laser. The energy generated by the laser heats the powder and causes the sintering effect, finally dispersing into the powder bed. And due to the very low thermal conductivity of the polymer powder deployed, the part bed retains heat over a relatively long period of time.

Experiments performed with sample geometries have shown that shrinkage occurring in the SLS machine is dependent on time, temperature, and pressure, i.e. the weight of the powder in which the part is embedded. To be able to calculate and compensate for shrinkage, it is important to ascertain the values of these three factors [14].

Another source of distortion in the production of objects by SLS is undesired growth of the part being produced beyond the volume defined by the laser beam. As is well known, the spot size of a laser beam can be made quite small so that the resolution of features in the object can be quite sharp. However, conduction of heat from fused locations can cause powder outside of the scan to sinter to the directly sintered portion causing the fused cross-section to grow beyond the area of the laser scan and thus beyond design dimensions. Growth can also occur from layer to layer if sufficient heat from

sintering remains in the fused portion that newly dispensed powder (in the next layer) sinters to the prior layer as it is dispensed [13].

Another factor to be considered is density. As the powder temperature within the area of the cylinder part of the SLS machine is not uniform because of the nature of the powder bed heating temperature system, density of sintered parts being produced is affected, which in turn also affects the strength of the sintered parts. The variation of density with part bed temperature for nylon 12 is given by the figure.

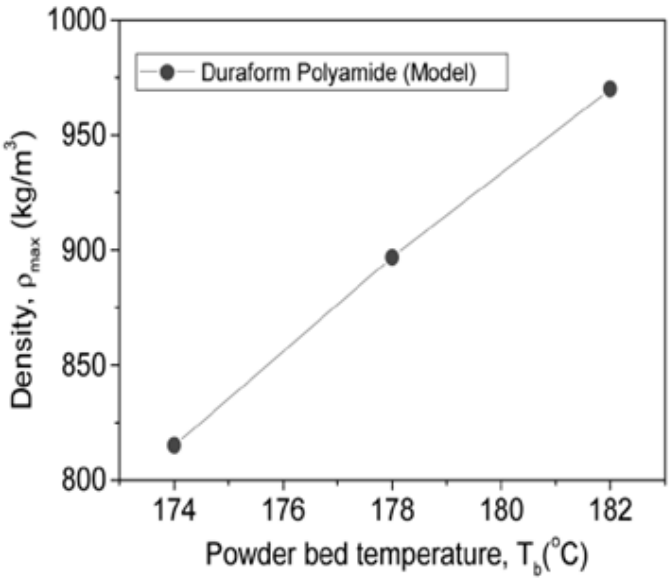

Figure 6 Density vs. Powder Bed Temperature of Duraform PA

Control of temperature of the sintered and unsintered powder at the target surface in the SLS is therefore important in minimizing such distortion in the object being

produced [13]. To maintain thermal homogeneity in the part bed, a radiant heater is suspended over the part bed to minimize the distortion effects of growth and curling of the part produced by the SLS process. Since the temperature of the surface of the part bed can change during the build cycle, feedback and control of the radiant heater may be included in the SLS machine. Usually this action is performed by an infra-red temperature sensor directed at target surface. Despite using a radiant heater for thermal homogeneity, inconsistencies have been observed in the formation of object cross-sections. Therefore it becomes essential to understand the thermal distribution inside the part bed which will facilitate better control of the system from a thermal standpoint [13].

Estimation of the temperature field in the powder bed in selective laser sintering is a key issue for understanding the sintering/binding mechanisms and for optimizing the technique. Heat transfer may be strongly affected by formation and growth of necks between particles due to sintering when the contact conductivity becomes predominant in the powder bed.

The various types of sintering mechanisms yielding powder binding depend strongly on temperature. This indicates that calculation of temperature fields in the powder bed in SLS plays a key role in understanding the operating sintering mechanisms (depending on the powder type and process parameters) and in estimating the binding kinetics. However, the associated heat transfer phenomena taking place in SLS process are complex including incident laser radiation penetration into the powder bed, thermal

radiation transfer, and thermal conduction through the gas filling the pores and through the contacts between the particles [15].

In most reported studies dealing with the SLS process, the modeling and simulation are usually limited to one- or two-dimensional analysis. For example, Nelson [16] used one-dimensional finite element and finite difference methods for density prediction for sintered amorphous polymer powders. Two-dimensional models were developed for the sintering of amorphous [17– 19] and semicrystalline polymers [20] to address the temperature gradient at part edges. A three-dimensional finite difference method was developed by Papadatos [21] to predict the density and temperature variation in parts built using amorphous polymer powders. Recently, Kolossov et al. [22] developed a three-dimensional finite element model for the simulation of temperature evolution during the SLS process for metallic materials. Dong et al. [23] developed a three-dimensional transient finite element model to simulate the sintering of semi-crystalline polymer powders, where temperature-dependent properties such as the thermal conductivity and the specific heat were considered. Not many studies on experimental temperature measurements of the SLS process have been conducted to understand the temperature distribution.

In the simulation work was done by Manetsberger, et al. [14], shrinkage in SLS was compensated by means of an FEM simulation which replicated the thermal conditions predicted within the build room during the building and cooling processes.

As shrinkage is a long-term effect, the highly dynamic effects of sintering were neglected when calculating the heat balance. Exposure of the part and the sintering process itself are instantaneous, i.e. time is not a factor in the transition from the initial density of the powder bed to the final density of the part. This simplification allowed them to select suitably large values for both the distance between nodes for the FEM simulation and the time intervals for the FEM calculation, thus greatly minimizing computation time.

Figure 7 depicts the thermal distribution inside the build chamber using the example of a hollow rectangular parallelepiped. For reasons of symmetry, only one-fourth of the build chamber is displayed in the figure.

Of course, the results of the shrinkage compensation are only as accurate as the thermal simulation itself; i.e. the actual temperature conditions in the build chamber must be simulated as closely as possible. For this reason the results of the simulation with empirical data were calculated. Since it was difficult to measure the exact temperature within a part, the temperatures within the powder bed near a sintered geometry were compared. The results are given by Figure 8.

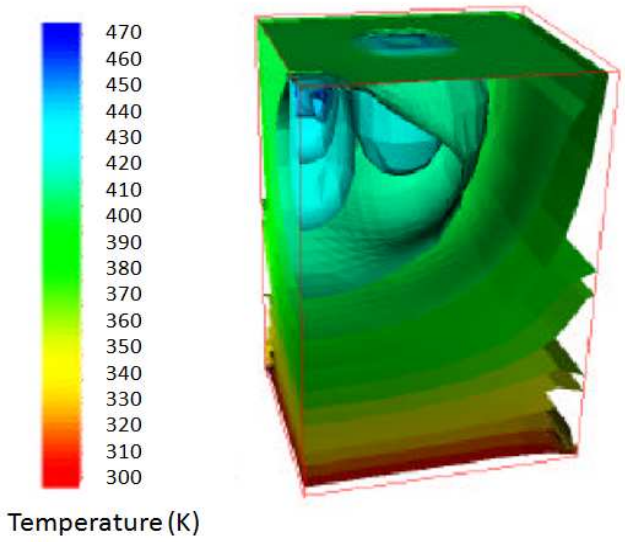

Figure7- Thermal distribution inside a SLS build chamber [14]

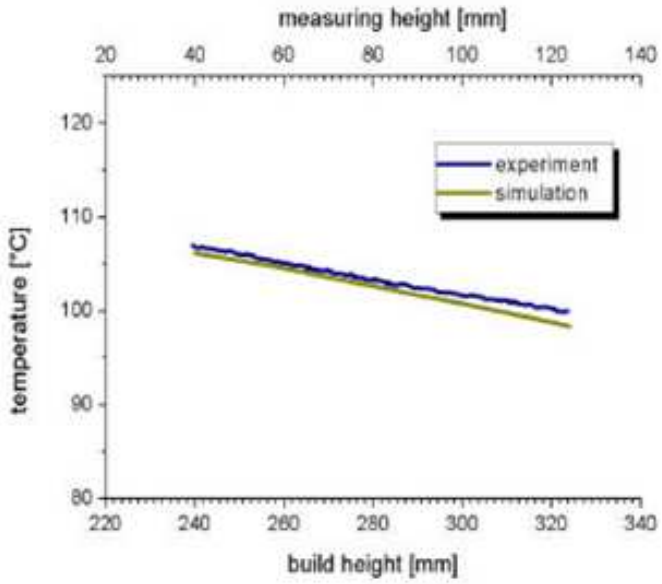

Figure 8-Comparison of temperatures measured during experiments and results of thermal simulation [14]

As expected, the height of the cylinder-shaped samples after shrinkage could be expressed as a function of the temperature and the pressure applied to the samples. When the final values of shrinkage and the temperature applied are expressed in the form of an Arrehnius plot, it becomes evident that the two values are linear in dependence. Thus, the dependency between temperature T and shrinkage S_{fin} may be expressed as follows:

$$\mathbf{S_{fin}} \ \alpha \ \mathbf{e}^{(-E/cT)}$$

with c=const. E may be understood as a thermal energy of activation: the higher the temperature, the greater the number of particle contacts which are thermally activated, with the result that a greater number of particles become active, sliding to fill the empty spaces. This increases shrinkage and subsequently the final density.

Figure 9 shows the shrinkage curves of a Poly (methyl methacrylate) (PMMA) sample sintered at a temperature of 140^{o}C and a pressure of 18.5 g/cm^{2}. Figure 10 is a schematic sketch illustrating the shrinkage mechanism for laser-sintered polymer samples, and Figure 11 gives the final corrected relationship between shrinkage and temperature.

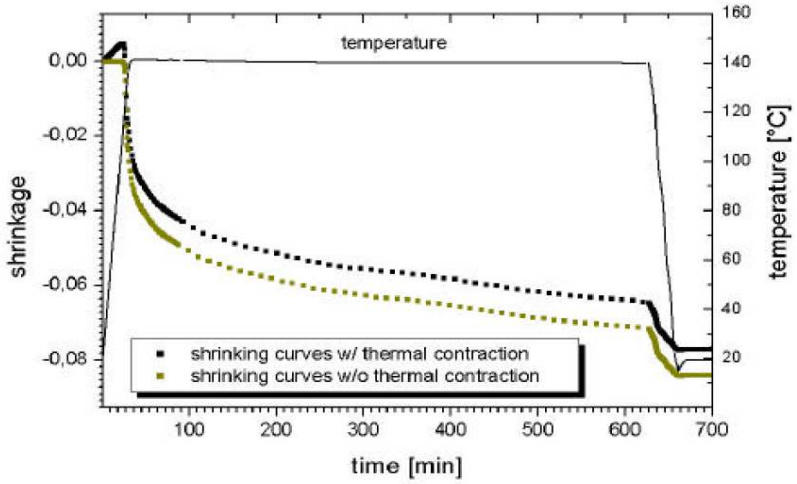

Figure 9- Shrinking curves of a PMMA sample sintered at T=140°C and p=18.5g/cm^2 [14]

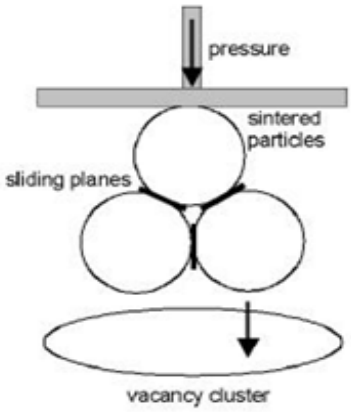

Figure 10- Schematic diagram illustrating the shrinkage mechanism for laser-sintered polymer samples [14]

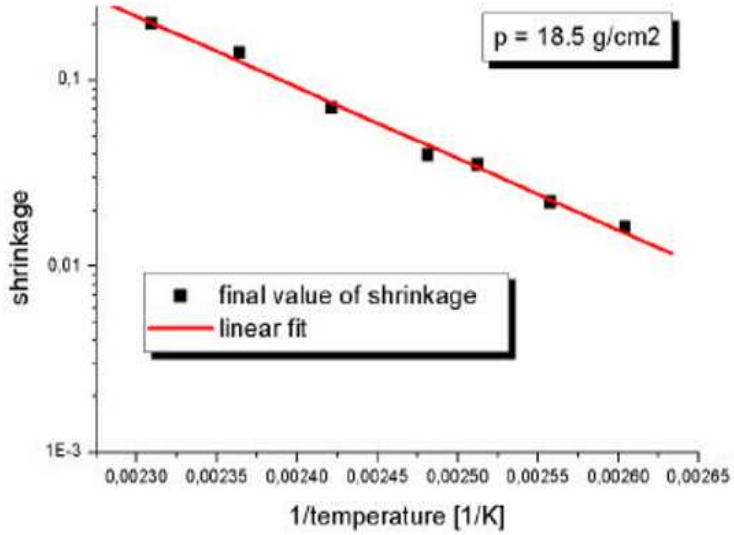

Figure 11-Temperature-dependency of the final values ascertained for shrinkage of parts [14]

The primary objective of this research study is to understand the thermal gradients in the part bed along X, Y and Z directions for selective laser sintering of Nylon-12 and to provide inputs to improve the thermal management of SLS, thereby improving part quality of products. For the temperature measurement of the build chamber, resistance temperature detectors (RTDs) were embedded in the part bed at varying locations.

Experiments were repeated with the RTDs being placed at various locations of the piston plate. Components of a typical SLS machine are shown in Figure 12.

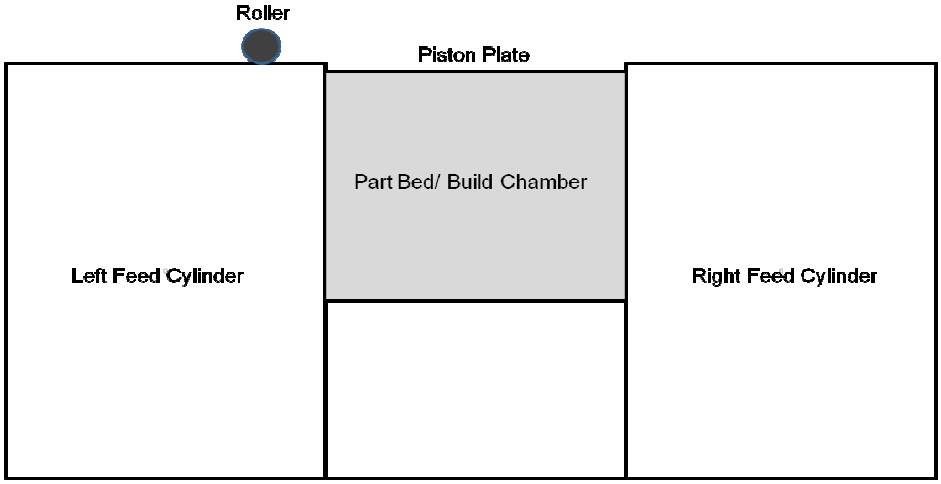

Figure 12- Components of an SLS system

Chapter 2

EXPERIMENTAL SETUP

2.1 Machines Used

Two SLS machines were used for conducting experiments as shown in Figure 13.The machine used for the sustainability study was the SLS Vanguard™ HiQ+HS and the machine used for the thermal distribution study was the DTM Sinterstation® 2500^{plus}.

Figure 13 A- SLS Vanguard™ HiQ+HS Machine [24]

Figure 13 B- DTM Sinterstation® 2500^{plus} Machine [25]

2.2. Sustainability Study

Two "full chamber build" prosthetic parts were built in this experiment. The CAD images of the parts are given by Figures 14 and 15. Part 1 had a volume of 0.000837567 m^3 and part 2 had a volume of 0.000840744 $m^{3.}$ The two parts were oriented in the part build of the machine as shown in Figure 16.

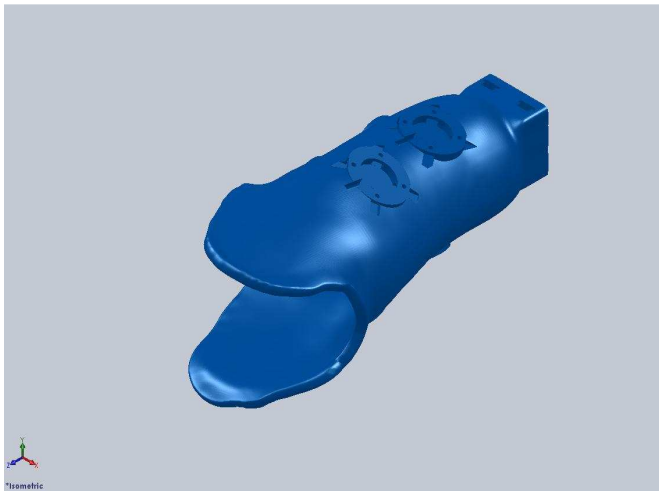

Figure 14- CAD image of Part 1

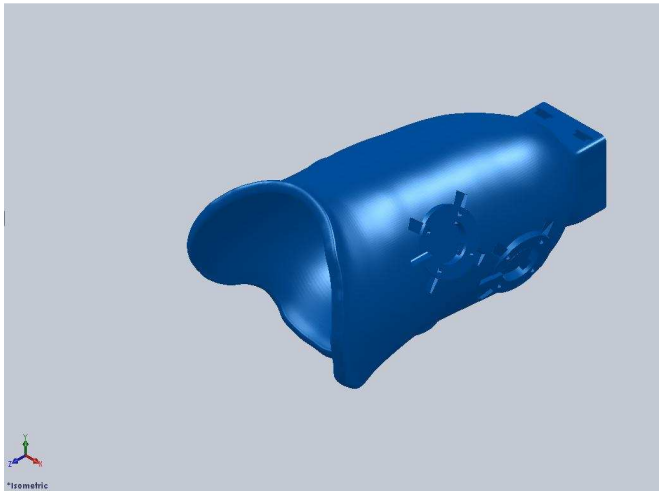

Figure 15- CAD image of Part 2

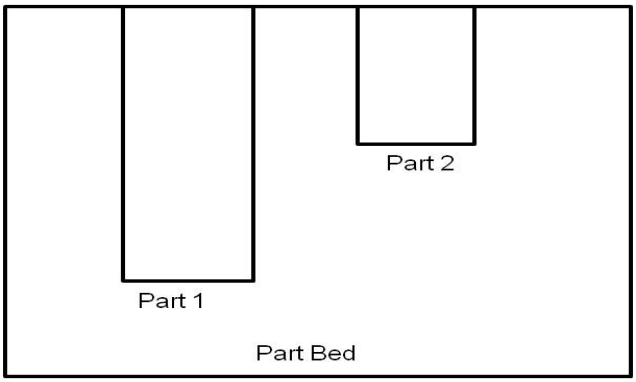

Figure 16- Orientation of Parts in the Build Chamber

The SLS Vanguard™ HiQ+HS machine was operated with the following parameters: the laser scan speed was 10 m/s; the powder layer thickness was 0.15 mm; the laser power was 50 W. The warm up height was 12.7 mm; the build height was 340 mm; the cool down height was 2.5 mm. All four heater zones were initially set at 100^{o} C. The part heater had a build zone temperature of 186^{o} C, and the right feed heater and left feed heater were set to 142^{o} C. The part cylinder heater zone had the lowest build zone temperature of 138^{o} C. The cool down zone temperature of both the feed heaters was 45^{o} C, whereas the part heaters had a temperature of 60^{o} C.

Technology used	Selective Laser Sintering
Power Source	Laser
Laser Type	50 W CO2
Laser Scan Speed	10000 mm/s
Maximum Build Envelope	370 x 320 x 445 mm
System Power	240 V AC, 3 phase, 50/60 Hz
CAD file needed	.stl

Table 3 - SLS Vanguard™ HiQ+HS machine specifications [24]

Heater Sytem	Temperature (^{o}C)		
	Warmup Zone	Build Zone	Cool Down Zone
Left Feed Heater	100	142	45
Right Feed Heater	100	142	45
Part Cylinder Heater	100	138	60
Part Heater	100	186	60
Powder Layer Thickness (mm)	0.15		
Laser Power(W)	Fill Laser Power-42.6		Outline Laser Power-5
Laser Scan Speed (m/s)	10		
Material Used	Duraform PA(Nylon 12)		

Table 4- SLS Vanguard™ HiQ+HS machine parameters used

Table 3 gives a list of the machine specifications. Table 4 summarizes the parameters used for the build. The major power drains of the SLS Vanguard™ HiQ are represented by Figure 17.

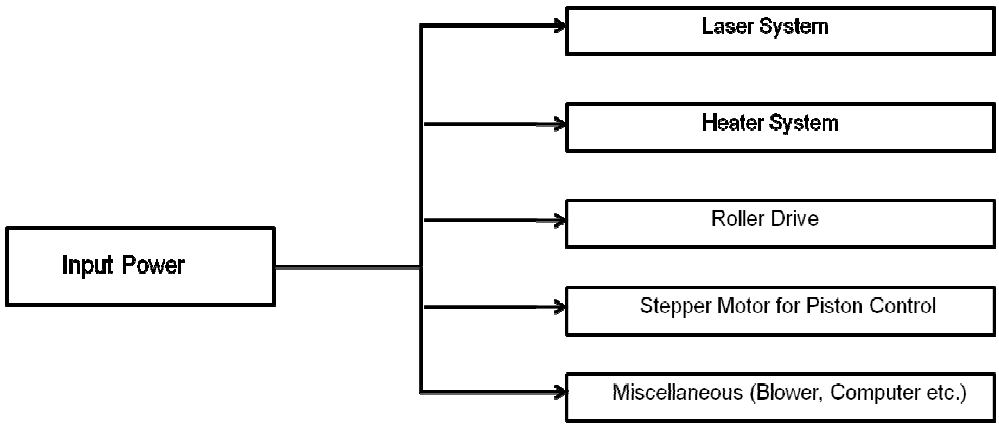

Figure 17- Power drains of the SLS Vanguard™ HiQ+HS Machine

Three Dranetz TR2013 clamp-on current transformers as shown in Figure 18 were used to measure the currents flowing across each channel of the input electrical connections to the three-phase ac machine. The current clamps had a rating of 100 Amperes (RMS Value). A LabVIEW circuit was designed to acquire the power data over lengths of time from the start to the end of the build. A NI-DAQ USB 6251 device was used as the DAQ (Data Acquisition) interface to gather the data. The sampling frequency was set in such a way that data were collected every two minutes from the start to the end of the build. This enabled acquisition of enough data to observe the trends in power

consumption during the various stages of the process. The same method was used to measure the power consumption of individual subsystems.

Figure 18- Dranetz TR 2013 Clamp-On Current Transformer

2.3 Thermal Distribution Study

Two experiments were conducted to determine the thermal profile of the part build in a DTM Sinterstation® 2500^{plus}. The first experiment involved building a perforated box of DuraformPA as shown by the Figure 19.

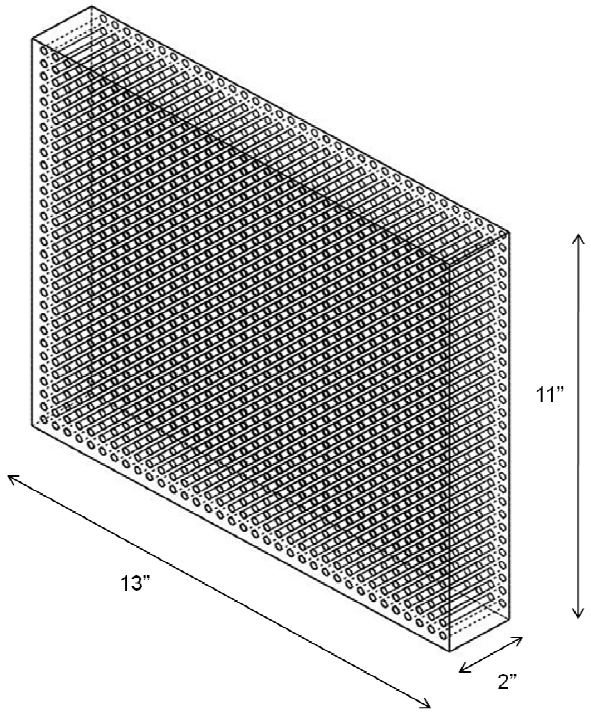

Figure 19- Perforated Box

The second experiment involved just depositing layers of powder for the build volume of 13" x 11" X 2" and allowing the temperature of the layers to get to the temperatures as programmed into the machine. The parameters used for both the builds are given by Table 5

Heater Sytem	Temperature (^{o}C)		
	Warmup Zone	Build Zone	Cool Down Zone
Left Feed Heater	80	80	45
Right Feed Heater	80	80	45
Part Heater	100	173	50
Powder Layer Thickness (mm)	0.10		
Laser Power(W)	Fill Laser Power-3.6	Outline Laser Power-4.0	
Laser Scan Speed (m/s)	5		
Material Used	Duraform PA(Nylon 12)		
Maximum Build Envelope	381 x 350 x 457 mm		

Table 5- DTM Sinterstation® 2500^{plus} machine parameters used

This research study was focused mainly on the internal thermal profile than the surface profile. The instruments used for temperature measurement were Resistance Temperature Detectors (RTDs). RTDs are temperature sensors that exploit the predictable change in electrical resistance of some materials with changing temperature [1]. The RTDs used for this research were Class A RTDs F3105 [26] made of platinum. Figure 20 A shows an RTD used for the experiments. The RTDs had a sensitivity of 0.00385 ohms/^{o}C. The configuration consisted of four wires and had an operating range of -70^{o}C to 600^{o}C. The RTDs were hooked up to a data acquisition (DAQ) device and

then operated by a LabVIEW circuit. The DAQ device used was the NI 9217 with four channels specifically designed to acquire analog data from 3 and 4 wire RTD configurations [27]. A NI 9217 DAQ device is represented in Figure 20 B.

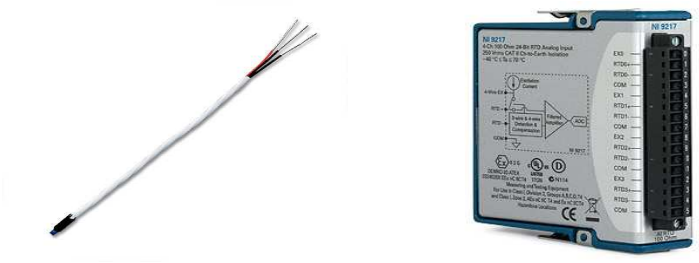

Figure 20 A- F3105 4 wire RTD B- NI 9217-DAQ Device

The setup used for the experiments is given by Figure 21. Two RTDs were used for the experiements. One was fixed at the center of the piston plate. The other one was installed at the right corner of the plate. The arrangement of RTDs on the piston plate is shown by Figure 22 . The RTDs were buried in the powder bed and fixed with respect to the piston plate. As the piston dropped down during the course of the experiment, so did the RTDs.

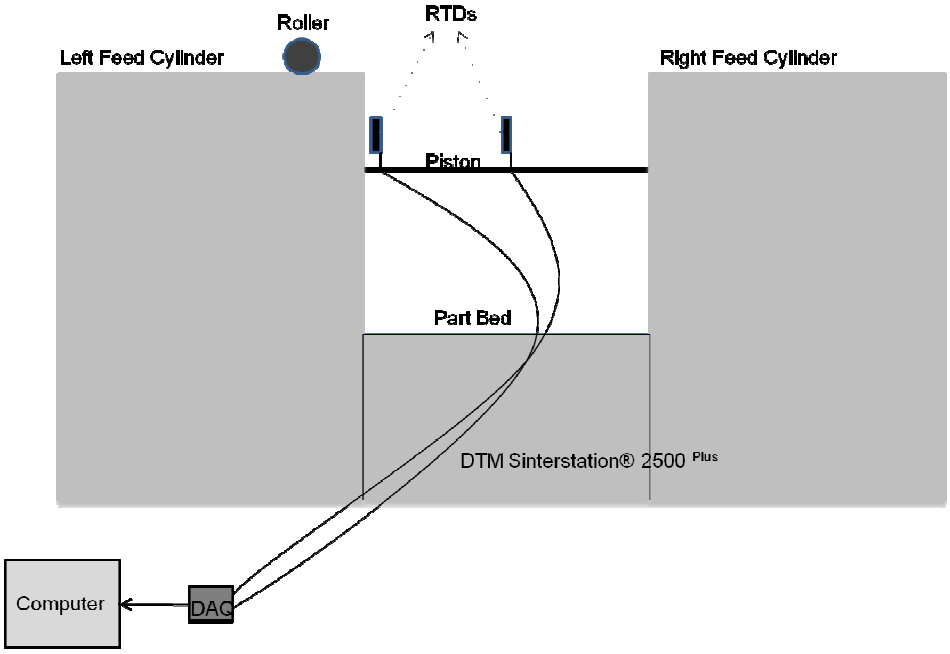

Figure 21- Experimental Setup for Internal temperature measurements

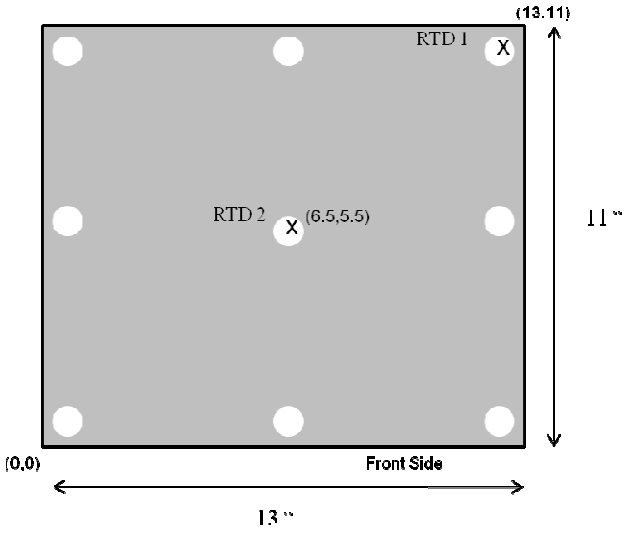

Figure 22-Arrangement of RTDs on the Piston Plate, denoted by "X"s

Chapter 3

RESULTS

3.1 Sustainability Analysis

A warm-up layer of 0.5 inches Nylon-12 powder was deposited and brought to 100^{o} C. Then successive layers of 0.004 inches were deposited, brought to 186^{o}C and then sintered. The whole build took about 12.5 hours. The clamp-on ammeters were clamped to the machine for the whole length of the build. Figures 23, 24 and 25 give the current flowing across the three phases of the machine plotted against time for the build of the prosthetic parts.

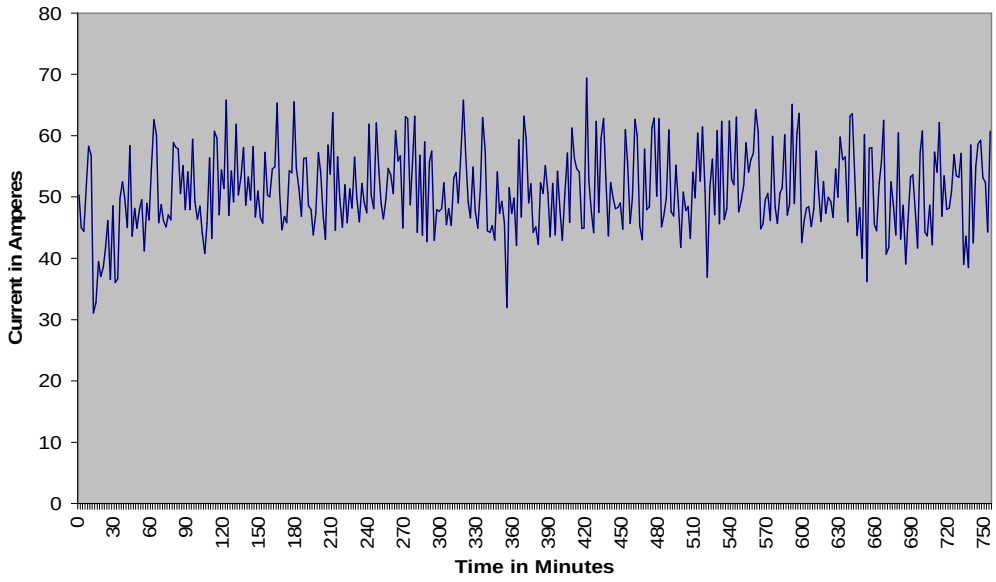

Figure 23-Current versus Time in Phase 1

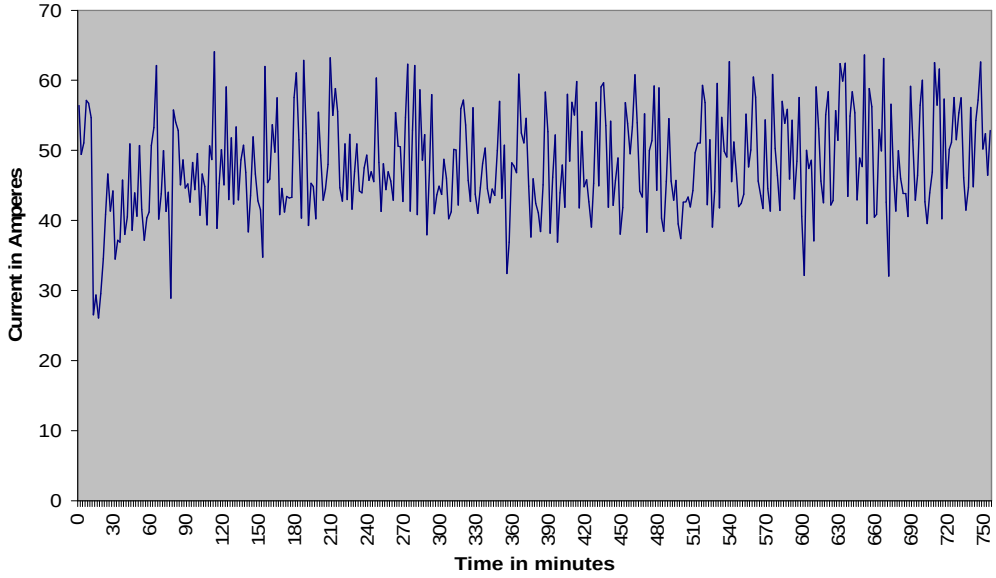

Figure 24-Current versus Time in Phase 2

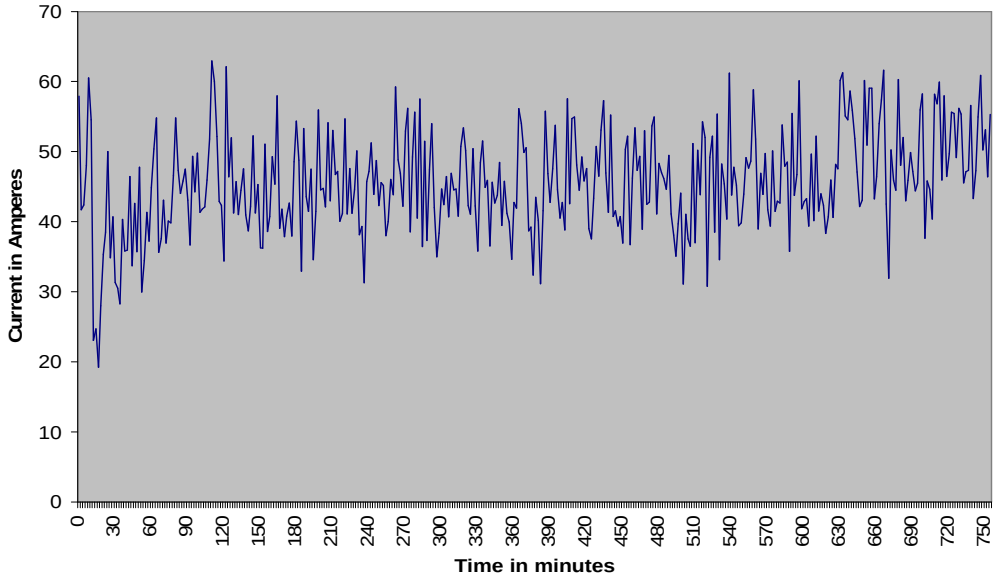

Figure 25-Current versus Time in Phase 3

From the graphs, the average values of current flowing across the three phases were calculated to be 51 A, 47.99 A and 45.6 A, respectively. The line voltage (V_L) of the system is 235 V. Therefore the power of the system can be calculated as follows [28]

$$\text{Power (W)}, P = (V_L/\sqrt{3}) * (I_1+I_2+I_3) \quad (1)$$

Where I_1, I_2 and I_3 are the currents flowing in phase 1, phase 2 and phase 3 respectively. From the aforementioned values of currents and voltage, the power was calculated to be 19.6 kW. However this is the average power value obtained during the entire build. The original power values were found to vary from 10 kW to 24 kW as shown in Figure 26.

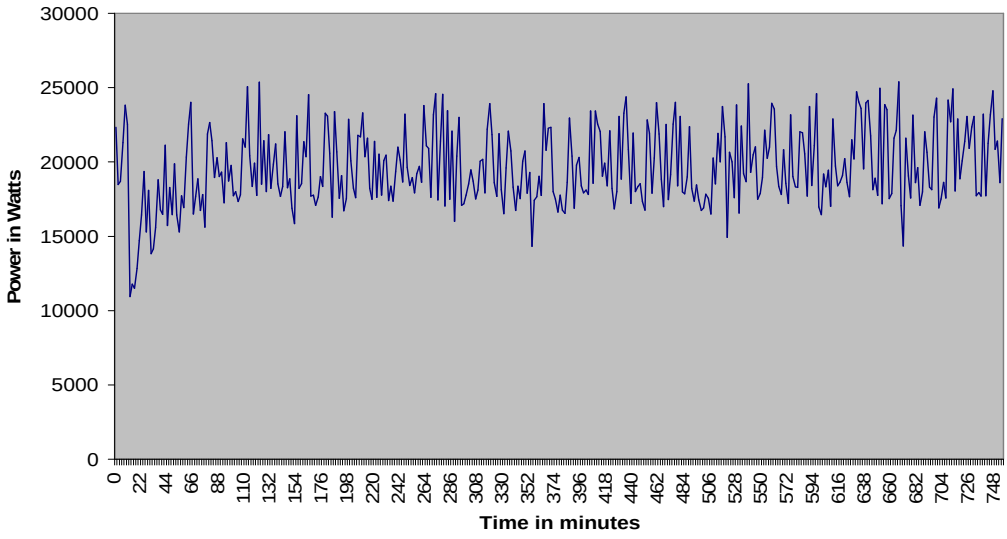

Figure 26-Power drawn by the machine versus Time

The power drawn by various drains were also calculated and it was found out that the heater system which is used for heating the powder bed was the biggest accumulator of electricity followed by the stepper motor system which controls the piston motion of the powder bed, then the roller system which spreads the powder across the bed and finally the laser system. The difference between the total power and the power acquired by individual components was attributed as unaccounted losses which included the computer interface, the blower system, etc. The approximate values of power acquired by the individual components are given below in Figure 27.

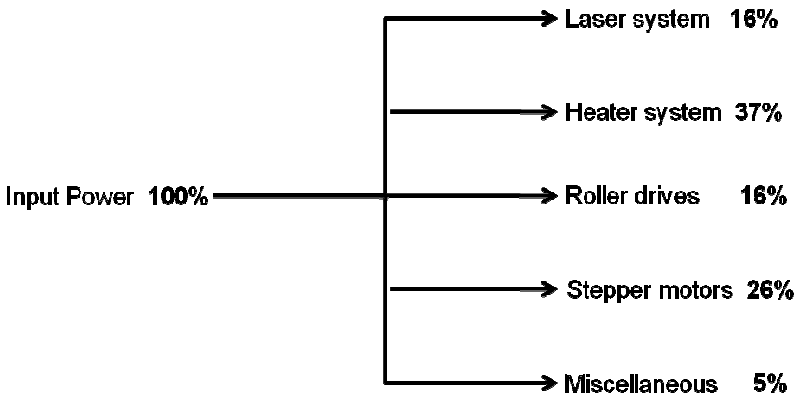

Figure 27-Power drawn by Individual Components

3.2 Thermal Distribution

3.2.1Sheet of paper build

The internal temperature measurements were tested during the fabrication of a “sheet of paper (25.7 X 17.2 cm)". A pair of RTD's was embedded in the part bed, one near the center and one near the right rear corner, 1 inch (25.4 mm) above the piston surface, and ½ inch (13 mm) below the surface. A time history of the RTD signals and depth below the powder surface was plotted and is shown in Figure 28.RTD1 represents the RTD placed at the corner of the piston plate, and RTD2 represents the one placed at the center of the piston plate. The machine was preheated to 80^{o}C overnight. ½ inch (13 mm) of powder was deposited during the normal warm-up cycle, in which the part bed surface was heated to 173^{o}C before each successive 0.004 inch (0.1 mm) layer of powder was deposited. To heat the first layer during the warm-up required about 18 minutes. The remainder of the warm-up layers was deposited over the subsequent 68 minutes. One layer of powder was sintered in a 25.7 X 17.2 cm sheet, over 9 minutes. Then 0.1 inches (2.54mm) of powder was deposited on top of the sintered sheet in 0.004 inch (0.1 mm) layers, and the machine was allowed to cool down.

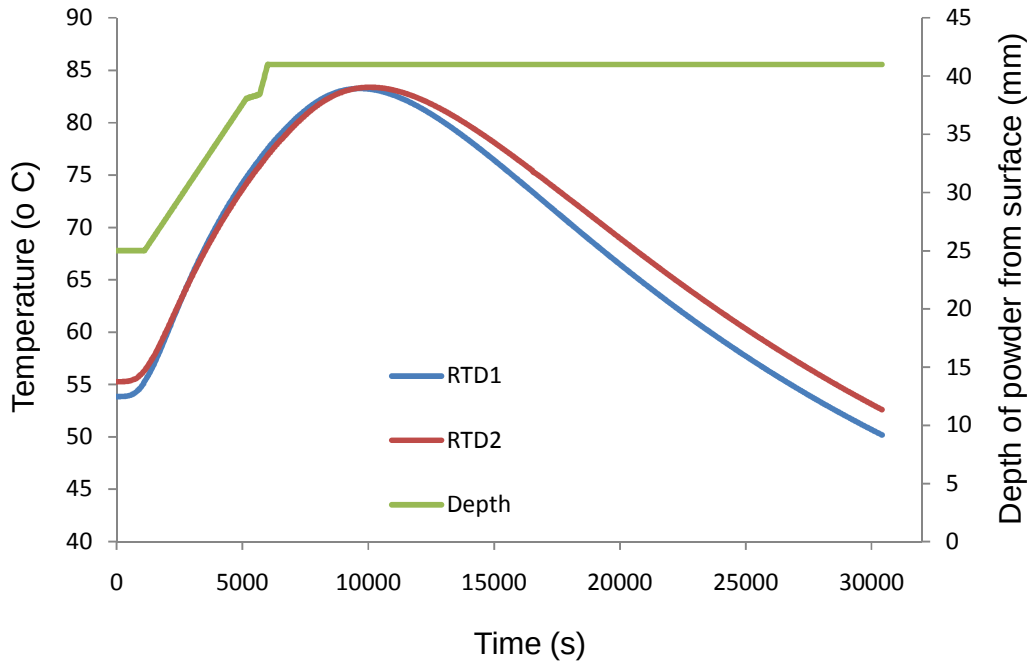

Figure 28- RTD readings of temperature for the sheet of paper build

3.2.2 Perforated box build

Figure 29 shows the temperature distribution for the perforated box build. A pair of RTD's was embedded in the part bin, one near the center and one near the right rear corner, 1 inch (25.4 mm) above the piston surface. The two RTDs were placed 0.005 inches (0.127 mm) below the surface of the part bed. There were no warm-up layers deposited and the first layer was sintered as soon as the first layer deposited was brought to a 173^{o} C set-point. A single layer took approximately 9 minutes to sinter. 2 inches (50 mm) of the part was built by laser sintering of layers of 0.004 inches (0.1 mm) deposited

over one another. After the sintering process was complete, cool-down of the build started with no cool-down layers being deposited. The total build was completed over a period of 72 hours.

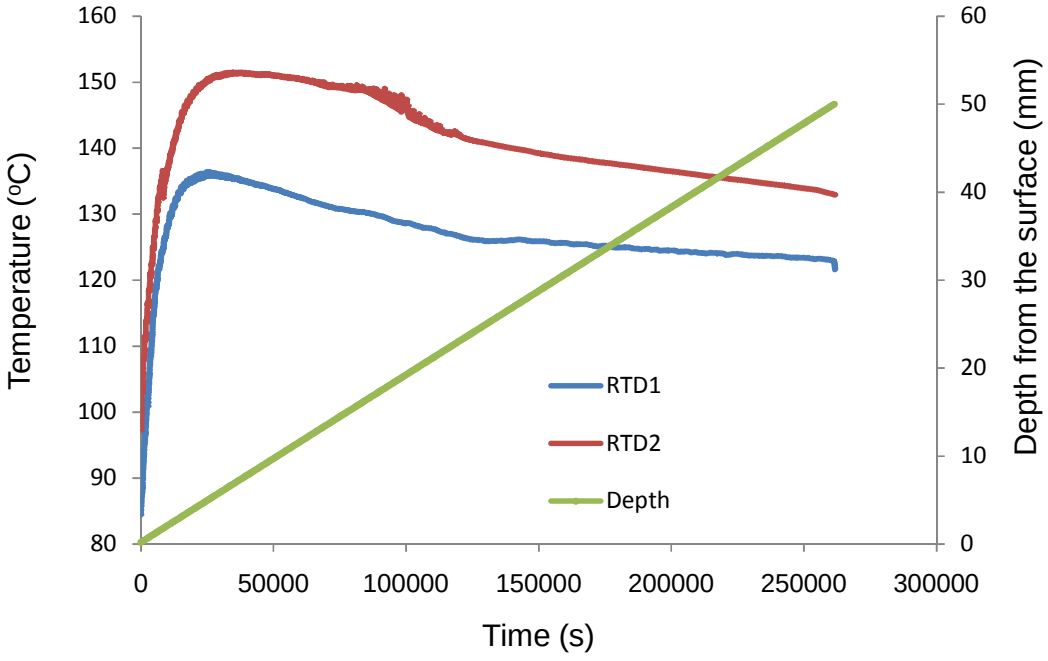

Figure 29- RTD readings of the perforated box build

3.2.3 Warm-up deposition

Figure 30 represents the temperature distribution of a warm-up layer deposition. 0.004 inches (0.1mm) of powder were deposited in layers for 2 inches (50mm) and allowed to reach the 173^{o} C set-point. No laser sintering was carried out. This experiment

was carried out to determine the effects of laser sintering on the temperature profile of the part build. The total time taken for the warm-up layer deposition was about 5.5 hours as opposed to the perforated box build which took about 72 hours.

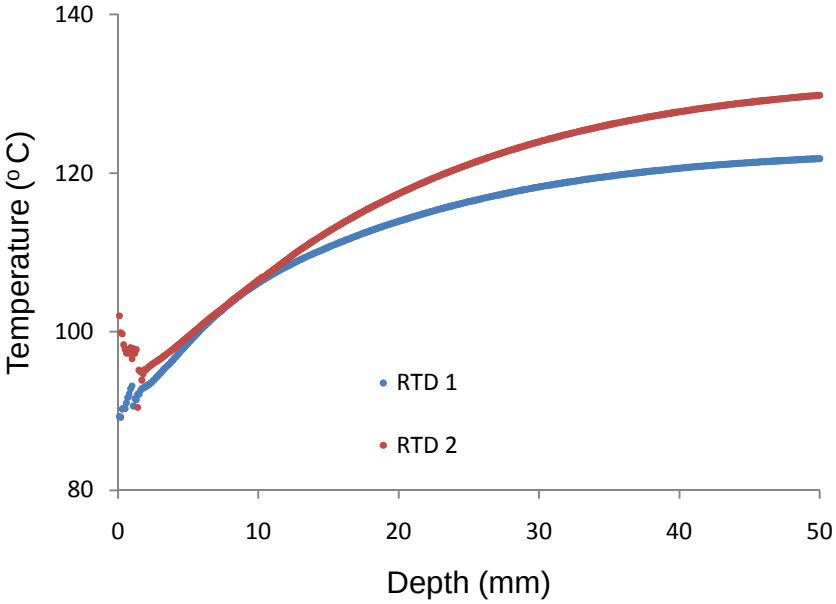

Figure 30- RTD readings of warm-up layer deposition

Chapter 4

DISCUSSION

4.1 Sustainability Analysis

4.1.1 Power Consumption Trends

Heating, which normally is considered a power intensive process, is done by four heater systems in an SLS Vanguard^{TM} HiQ+HS machine: left feed heater, right feed heater, part cylinder heater and part heater. The power consumed by the heater zones accounted for a significant portion of the total power consumed by the machine. The high power consumption of the stepper motor system was attributed to the reciprocating action in lifting heavy loads of powder on the feed cylinders. The laser system accounted for 16% of the overall consumption. The chiller setup which is used to cool the laser in an SLS machine uses an independent source in the case of a Vanguard^{TM} HiQ+HS machine. It consumed about 1.5 kW power. This value was not used in the sustainability analysis although a comprehensive study on sustainability of a process needs to include it.

4.1.2 Sustainability Indicators

Measures of environmental impact for certain materials, energy, etc. are needed to perform a sustainability analysis to determine the total energy factor. Environmental and Resource Management Data (ERMD) define what the environment actually is and how to quantify the consequences of impairment of the environment. In this study, the

ERMD data, Eco-indicator 95, collected and calculated by PRe Consultants of Netherlands [29] were used. The higher the indicator, the greater is the environmental impact. The principle of Eco-indicator is explained by Figure 31. The eco-indicator for a certain material or a process can be obtained as follows. First, inventory of all environmental effects and damages are made. Then a normalization is applied to obtain some equivalent effects. Finally weighting factors are used to scale the effects.

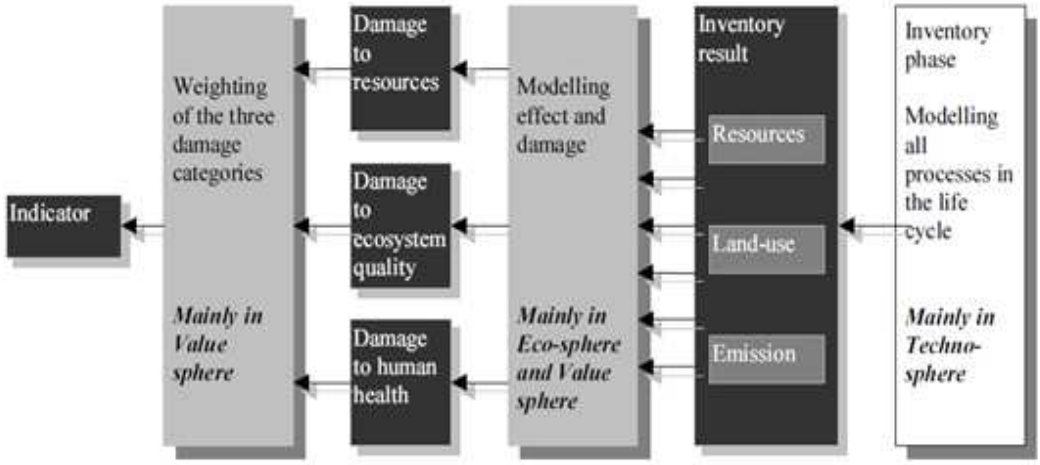

Figure 31- Principle of Eco-indicator [29]

Luo, et al. [5] devised a process model to compare the total energy factors of several SFF processes. The ERMD data, the Eco-indicator 95, was employed to provide quantitative measures for the total energy consumed during the process.

For the analysis, the following process parameters were used: V, scanning speed (mm/s); W, road width size (mm); T, layer thickness (mm); ρ, material density (kg/mm3); P, power rate (kW); and k, process overhead coefficient (0.6-0.9).

The Process Productivity (PP) and the Energy Consumption Rate (ECR) may be determined according to the principle of layered fabrication as

$$PP\ (kgh) = V \times W \times T \times \rho \times 3600 \times k \qquad (2)$$

and

$$ECR\ (kWhr/kg) = \text{Power rate} / \text{Process Productivity} \qquad (3)$$

The total energy indicator was obtained by the product of ECR and Eco-Indicator for electricity which is 0.57 [29]. The specific gravity of Nylon-12 was taken as 1.04.

Table 6 shows the total energy indicator of SLS Vanguard^{TM} HiQ. The overhead factor was taken as 0.6 [5]

Parameters	SLS Vanguard™ HiQ
V (mm/s)	10000
W	0.4
T	0.15
Specific gravity	1.04
K	0.6
P (kW)	19.6
Process productivity(kg/hr)	1.35
Energy consumption rate (kWhr/kg)	14.5
Eco-indicator (/kWhr)	0.57
Total Energy Indicator	**8.3**

Table 6- Sustainability Analysis of SLS Vanguard™ HiQ

The Total Energy Indicator value for the SLS Vanguard™ HiQ sinterstation with Nylon-12 was calculated to be approximately 8 which compared competitively with that

of Stereo Lithography SLA®5000 and Fused Deposition Modeling FDM-8000 which were 12 and 13, respectively [5]. Therefore on an energy consumption perspective, SLS fared much better than the other two SFF processes.

The mean power consumed by the HiQ+HS machine was about 19.6 kW. The energy consumption rate as given by Table 6 was calculated to be 14.5 kWhr/kg [ECR]. This value is less compared to the one published by researchers at Loughborough University [30]. Their value of ECR was 56 kWhr/kg. The reason for this discrepancy might be that the process productivity was assigned a much smaller value in their study. The value used in our study was 1.35 kg/hr. This value was derived from Luo et.al [5]. Baumers, et al. [30] also report a lower value for mean power consumption at 4.7 kW for an SLS VanGuard HiQ+HS™ machine. The instrumentation used to measure energy consumption in their study was a portable power monitoring setup based on Yokogawa's CW240 digital power meter [30]. The instrument used for our study was a clamp-on ammeter which recorded instantaneous current readings which were then multiplied with the line voltage (V_L) as shown in Eq.(1). The difference of about 300% in power readings in both cases is attributed to instrumentation errors.

4.2. Thermal Distribution

4.2.1 Material Properties

Understanding the material properties was important for determining the thermal characteristics of the SLS machine.

Density (ρ) is one key property that governs sintering of a powder system [31]. The density of the Duraform PA^{TM} powder was measured by building a cubic shell and carefully measuring its mass and volume. The cube was emptied and carefully cleaned, and the shell's mass and internal volume were measured again. The density of the powder in the cake surrounding a sintered part was found to be 490 kg/m^3. This represents the density of the powder system while in the machine. A density of 1010 kg/m^3 was used for the density of solid nylon.

Porosity (ε) can be defined as

$$\varepsilon = 1 - (\rho_{powder} / \rho_{solid}) \qquad (4)$$

Thus by substituting the values of density, the porosity of the powder used is calculated as 51%.

Thermal conductivity is much more complex to determine as several approaches have been used to form an effective thermal conductivity, k_{ef}, for SLS powders [15, 23,

32, 33] and each of them give different results. Dong et al made an estimate based on porosity, shown in Eq (5). [23]

$$k_{ef} = k_s (1- C\varepsilon) \quad (5)$$

where $k_s = 0.28$ (W/mK) is the thermal conductivity of the solid material, C = 1.11 is an empirical constant.

The method used by Gusarov, et al is based on thermal contact between spherical particles but does not account for the conductivity of the interstitial gas [15]. The estimate of k_{ef} is given in Eq (6).

$$k_{ef} = k_s (pn/\pi) \quad (6)$$

where p is the relative density, p = 1-ε, n is the coordination number based on the packing configuration, and x is the contact surface ratio, x = a/R, where a is the radius of the circular contact region between particles, and R is the particle radius. The relative density for nylon-12 powder in this study was p = 0.49 which fell between the calculated relative densities for simple-cubic and diamond packing configurations. The coordination number was estimated by performing a linear interpolation based on the relative densities and coordination numbers of the simple cubic and diamond packing configurations to find $n_{est} = 0.88$.

By this method, k_{ef} is dependent on the contact surface ratio, which was unknown at the time of the study

$$k_{ef} = 0.88 k_s x \quad (7)$$

This relation is valid for $0 < x < 0.3$, which is given as a reasonable range for non-sintered powders. Thus, a reasonable upper limit on k_{ef} by this method is $k_{ef} = 0.074$ W/mK. The contact surface ratio increases during heating as the powder particles deform and begin to sinter, so that the conductivity may be much lower at the beginning of the build than it is at the end.

Nitrogen gas was used as the inerting medium in the SLS machine. A reasonable lower limit for k_{ef} would be the thermal conductivity of the interstitial gas $k_{N2} = 0.033$ (W/mK).

The specific heat of c = 1800 J/kgK was assumed to be the same for powder and solid nylon.

4.2.2 Thermal Profile of the part bed

4.2.2.1 Sheet of Paper Build

Figure 28 gives the RTD readings of temperature distribution inside the part bed of a "sheet of paper" build. There was a warm-up layer of 0.5 inches above which layers of powder were sintered. The temperature of the part heaters was set at 173^{o} C. However the highest temperature recorded by the RTDs was approximately 82^{o}C. This discrepancy is attributed to the poor thermal conductivity of the powder used.

Figure 32 is a numerical model that gives temperature contours of the machine as seen from the front view of the build chamber at the end of a simulated warm-up cycle. The three blue bins at the bottom are the powder bins. The space above the powder bins is N_2 in the range 400-450K (127-177^{o}C). The two hot spots in the center are the radiant heaters, at steady-state at this point in the simulation. The feed bin heaters are not energized because the surface temperature of the feed bins is at or above the set temperature.

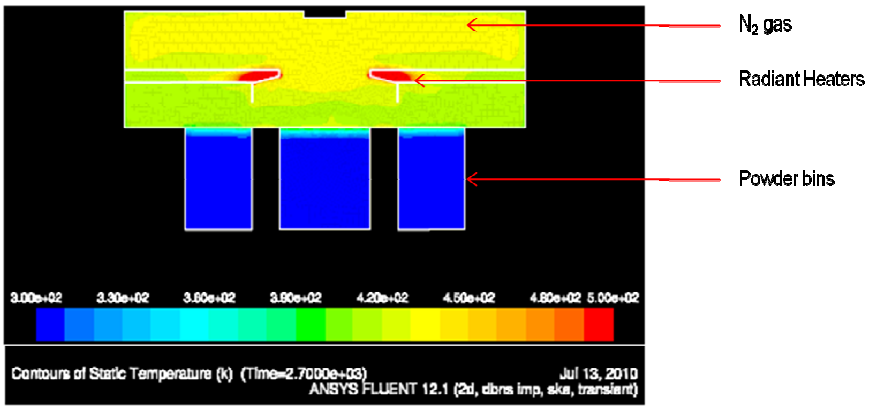

Figure 32- Temperature profile of 2-D numerical model at the end of simulated warm-up to 451K (178^{o}C)

Figure 33 is an infra-red image of the part bed surface. Measurements of the temperature at the surface of the part bed were made by means of an infrared (IR) camera. The camera was a FLIR model A325 thermal imaging camera, with a 320X240 pixel resolution and 16-bit resolution. The maximum temperature as recorded by the

camera on the surface is about 450 K (177^{o}C). This is in contrast to the readings of the RTDs which showed a maximum temperature of around 82^{o}C. At this particular time in the build, the distance of the RTDs from the surface of the piston was about 0.505 inches. The thermal gradient is due to the high insulating capacity of the Duraform PA^{TM} powder. In Figure 33, the right end of the surface is significantly hotter than the left end. The reason for this difference was due to the fact that the part heater had several hot spots in the right end compared to its left end. The thermograph of the part heater is shown by Figure 34.

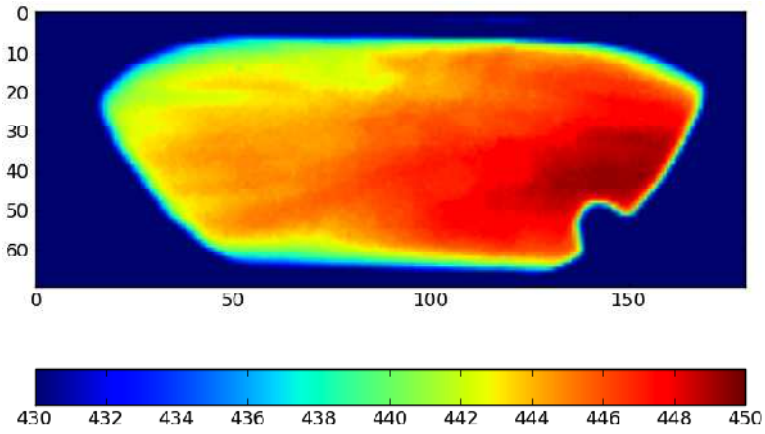

Figure 33- Thermal profile of the part bed surface during the sheet of paper build

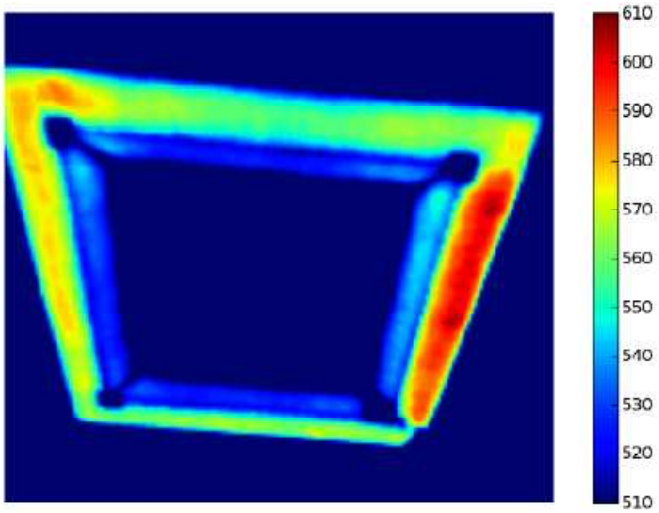

Figure 34- Thermal profile of the part heater

4.2.2.2 Perforated box build

The sintering action of the laser was not captured in Figure 33 because of the high reflectivity of the surface during sintering. To capture the sintering effect, it was decided to build a perforated box that enabled access to sintered as well as non-sintered powder in the same plane. Figure 35 shows an image captured during the sintering of one of the layers of the perforated box. The maximum temperature recorded in the layer other than at the point of impact of the laser was approximately 450 K (177^{o}C). There was again a similar trend of the right end of the surface being hotter than the left end as expected. However, during the perforated box build, the temperature of non-sintered powder read low compared to the sintered portion as shown in the figure. This is an indication that the laser action leaves behind a significant thermal print.

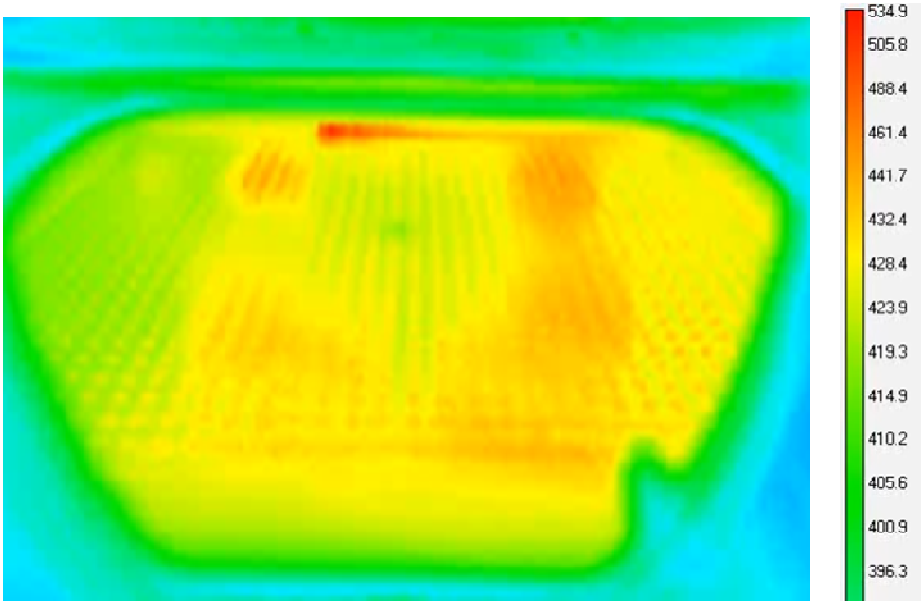

Figure 35- Thermal profile of part bed surface during the first layer of the perforated box build

This trend however, disappeared with further addition and sintering of layers. An image recorded halfway through the build (about 1 inch depth) showed no difference between the sintered and non-sintered powder. The thermal image was uniform throughout as shown in the Figure 36.

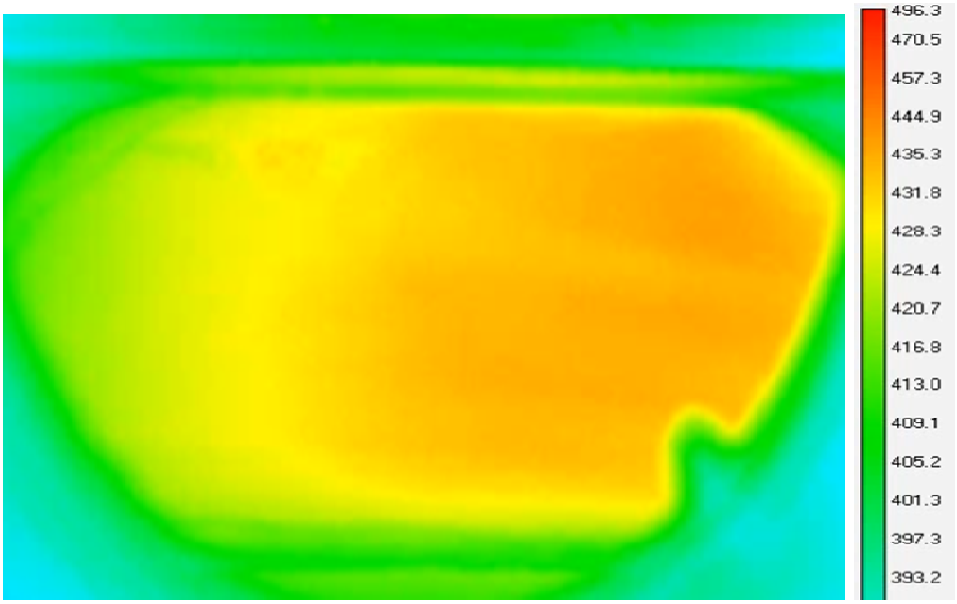

Figure 36- Thermal profile of the surface midway through the perforated box build

This build was carried out with no warm-up layers. The RTDs were embedded at 0.005 inches (0.127mm) below the surface. Therefore when the first layer was being sintered, the tip of the RTDs was 0.009 inches (0.23 mm) below the top of the surface. The highest temperature recorded by the RTDs was around 150^{o}C. There was a gradient of around 20^{o}C between RTD1 and RTD2. The lower temperature recorded by the RTD at the right corner (RTD1) was because of the proximity to the metallic part bin wall.

4.2.2.3 Warm-up layer deposition

Figure 30 gives the RTD readings when layers of powder were deposited and brought to 173^{o}C without laser action. The RTDs were again placed 0.005 inches below the surface. The temperature reached a maximum however as the depth of layers increased. This showed that in the absence of the laser action, the time taken for the temperature to reach steady state and to be conducted along layers was very high.

Chapter 5

CONCLUSIONS

5.1 Sustainability Analysis

Power consumption in a 3D Systems Vanguard™ HiQ+HS sinterstation was measured using Dranetz TR2013 clamp-on ammeters. For a Nylon-12 full chamber build, the average total power consumption was found to be 19.6 kW. Most of the energy was consumed by the chamber heaters (37%), followed by the stepper motors for the piston control (26%), the roller drives (16%) and the laser (16%). The chiller setup for a Vanguard™ HiQ+HS sinterstation uses an independent power source. It drew about 1.5 kW. Then a sustainability analysis was carried out using Eco-Indicator 95 which is a type of Environmental and Resource Management Data (ERMD). A Total Energy Indicator value was calculated from the various parameters involved such as power consumption, process productivity etc. The TEI of SLS, approximately 8.0 was found to be competitive with other additive manufacturing processes. The sustainability of the process can be improved by increasing productivity of parts produced. Energy savings which will also lead to an improvement in sustainability can be achieved by operating the build process at room temperature, although for materials like Nylon-12, part integrity will suffer.

5.2 Thermal Distribution Study

Resistance Temperature Detectors were positioned inside the part bed of a DTM Sinterstation® 2500^{plus} machine to determine the thermal profile of an SLS process. Temperature measurements in the powder cake around the part confirmed the low thermal diffusivity of nylon powder. It was interesting to note, for instance, that in the case reported in Figure 28, the machine had been left to warm up to 80^{o}C overnight. Although the interior space was at steady state, the initial temperature recorded by the RTD's was 25^{o}C below the surface temperature. The peak temperature reached at the surface during the build was 178^{o}C, yet the peak temperature recorded by the RTD was 91^{o}C lower. The lower temperatures recorded by the corner RTD are explained by its proximity to the part bin wall.

The results show that the implications for part quality are substantial. That is, monitoring and maintaining the radiant heaters was shown to be important for part quality as given by Figure 34.It was also confirmed that radiation dominated the heat transfer in the build chamber, and convection played a very minor role.

The effects of laser sintering also played a huge role in temperature distribution of the bed. A build without laser sintering, with the same parameters read 20^{o}C less than the one with laser action.

3. Future Work

- A life cycle analysis should be done to determine the comprehensive sustainability of the process. Primary refining of material, which is not considered in this study, usually consumes about 80% of the total energy involved in a manufacturing process [34].
- Infinitely recyclable materials and other ways to reduce material consumption should be investigated.
- New designs to improve productivity of the process need to be made to reduce the carbon foot print of SLS.
- A model should be developed to compare and quantify the sustainability of additive manufacturing and conventional manufacturing technologies.
- For better thermal management of SLS, the material properties need to be refined based on experimental results and further characterization.
- A systematic plan must be formulated to ensure proper maintenance of heater systems in the machine.

REFERENCES

1) James R. Mihelcic, John C. Crittenden, Mitchell J. Small, David R. Shonnard, David R. Hokanson, Qiong Zhang, Hui Chen, Sheryl A. Sorby, Valentine U. James, John W. Sutherland, Jerald L. Schnoor, Sustainability Science and Engineering: The Emergence Of A New Metadiscipline, Environmental Science and Technology, Volume 37, No.23, 2003, P.P 5314-5324

2) Meadows, DH, Meadows, DL, Randers, J & Behrens III, WW. The Limits to Growth (Universe Books, New York, 1972)

3) Subhas K. Sikdar, Sustainability Development and Sustainability Metrics, AIChE Journal, Volume 49 , No. 8,2003, P.P 1928-1932

4) Saling, P., C. Wall, R. Wittinger, and A. Kicherer, Eco-Efficiency: A Tool to Demonstrate the Sustainability of BASF Products, Conf. Proc. Sustainable Eng., S. K. Sikdar, ed., AIChE Meeting, Indianapolis, IN, 135 (Nov. 3-8, 2002).

5) Luo, Y., Leu, M. C., Ji, Z., and Caudill, R., Lifecycle Assessment of Solid Freeform Fabrication Processes, Proceedings of 6th International Seminar on Life Cycle Engineering, Kingston, Canada, 1999, pp350-360

6) World Commission on Environment and Development. Our Common Future; Oxford University Press: New York, 1987

7) Dahotre, N. B. & Harimkar, S. P. Laser Fabrication and Machining of Materials (Springer Science Business Media) ISBN 9780387723433, 2008.

8) Morrow W.R., Qi H., Kim I., Mazumder J. and Skerlos S.J., Environmental aspects of laser based and conventional tool and die manufacturing, Journal of Cleaner Production, Vol 15, 2007, pp. 932-943

9) Thiriez A., An environmental analysis of injection molding, Master's thesis, Department of Mechanical Engineering, Massachusetts Institute of Technology, Cambridge, MA, 2005

10) Burns M , Automated fabrication, PTR Prentice Hall, New Jersey, 1993

11) Luo Y., Ji Z., Leu M. C. and Caudill R., Environmental Performance Analysis of Solid Freeform Fabrication Processes, Proceedings of the IEEE International Symposium on Electronics and the Environment, 1999, pp 1-6

12) Tuck. C., Hague. R.J.M., Reeves. P., ATKINS feasibility study – Initial investigation into the use of Rapid Manufacturing as a sustainable alternative to traditional processes – available online at http://www.atkins-project.com/web/atkins/contacts.cfm

13) Beaman, Joseph J.; McGrath, Joseph C. "Thermal control of selective laser sintering via control of the laser scan." US Patent, US5352405, 1994.

14) Manetsberger, K., Shen, J., Muellers, J., Compensation of non-linear shrinkage of polymer materials in selective laser sintering. In: Solid Freeform Fabrication Symposium, 2001 pp. 221–232

15) Gusarov A.V., Laoui T., Froyen L., Titov V.I., Contact thermal conductivity of a powder bed in selective laser sintering, Int. J. Heat Mass Transfer 46 , PP 1103–1109, 2003

16) Nelson J. C., PhD Thesis, The University of Texas at Austin, 1993

17) Bugeda G., Cervera M., and Lombera G., Rapid Prototyping Journal, 5, 21 1999

18) Childs T. H. C., Berzins M. , Ryder G. R., and Tontowi A. E., Proc. Inst. Mech. Eng., Part B 213, 333, 1999

19) Williams J. D. and Deckard C. R., Rapid Prototyping Journal, 4, 90 1998

20) Tontowi A. E. and Childs T. H. C., Rapid Prototyping Journal, 7, 180 2001

21) Papadatos A. L., MS Thesis ,Clemson University, Clemson, 1998

22) Kolossov S., Boillat E., Glardon R., International Journal of Machine Tools and Manufacture, 44, 117 2004

23) Dong L., Makradi A., Ahzi S. and Remond Y., Three-dimensional transient finite element analysis of the selective laser sintering process, Journal of Materials Processing Technology,Vol.29,pp:700-709, 2009

24) http://www.3dsystems.com/products/datafiles/datasheets-1007/SLS/DS-Sinterstation_HiQ_US_0407.pdf

25) http://check.itgo.com/#sls

26) RTD F 3105 http://www.omega.com/Temperature/pdf/RTD-2-F3105.pdf

27) NI DAQ 9217 http://sine.ni.com/ds/app/doc/p/id/ds-193/lang/en

28) Stevenson, William D., Jr. Elements of Power Systems Analysis. McGraw-Hill electrical and electronic engineering series (3rd ed.). New York: McGraw Hill. ISBN 0-07-061285-4, 1975

29) PRe Consultants, Netherlands, The Eco-Indicator 95 Report, http://pre.nl/eco-indicator95/ei95-reports.htm

30) Baumers M., Tuck C., Bourell D., Sreenivasan R., Hague R., Sustainability of additive manufacturing: Measuring energy consumption of the laser sintering process, Proceedings of the Institution of Mechanical Engineers, Part B: Journal of Engineering Manufacture, 2010.

31) German, Randall M. Powder Metallurgy & Particulate Materials Processing. Princeton, NJ: Metal Powder Industries Federation, 2005.

32) Slavin, A., Londry, F., and Harrison, J., A new model for the effective thermal conductivity of packed beds of solid spheroids: alumina in helium between 100 and 500 c, International Journal of Heat and Mass Transfer, 43(12), pp. 2059-2073, 2000.

33) Slavin, A., Arcas, V., Greenhalgh, C., Irvine, E., and Marshall, D., Theoretical model for the thermal conductivity of a packed bed of solid spheroids in the presence of a static gas, with no adjustable parameters except at low pressure and temperature, International Journal of Heat and Mass Transfer, 45(20), pp. 4151-4161, 2002.

34) Bert Bras, Energy and Sustainability, Presentation at the Roadmap for Additive Manufacturing (RAM) workshop, Arlington, VA, March 30, 2009